# Vessel Relocation Solution for Steel Catenary Riser Touch Down Fatigue Management

**Achoyamen Michael Ogbeifun*[a], Selda Oterkus[a], Julia Race[a], Harit Naik[b], Dakshina Moorthy[c], Subrata Bhowmik[b], Julie Ingram[c].**

[a]Department of Naval Architecture, Ocean and Marine Engineering, University of Strathclyde, 100 Montrose Street, Glasgow, G4 0LZ, UK; [b]McDermott International, 40 Eastbourne Terrace, Paddington, London, W2 6LG, UK; [c]McDermott International, 757 N. Eldridge Parkway, Houston, TX 77079, USA.

**Corresponding author*; e-mail: achoyamen.ogbeifun@strath.ac.uk, phone: +44 7414 517 860

## ABSTRACT

This work is focused on developing a formal optimisation approach to the vessel relocation program for steel catenary riser (SCR) touch down zone (TDZ) fatigue management. Vessel relocation is the planned repositioning of the vessel within the acceptable limit of the riser design to help spread and reduce the fatigue damage over the SCR TDZ. There is a need to obtain an optimum vessel relocation program that best reduces the SCR TDZ fatigue damage. Hence, the facility operator will need to know the optimum combination of the following: the number of stations along the relocation axis, the distance limits for the relocation, and the relocation axis direction. The constraints on the problem are imposed by the stress utilisation, TDZ compression and top tension. The index-matching optimisation technique is applied to solve the optimisation problem. To demonstrate the approach's suitability, we consider a single SCR hosted by a production platform. The fatigue damage responses of the SCR with the optimum vessel relocation programs are compared with those without vessel relocation. The results obtained indicate that a considerable fatigue reduction can be achieved through a well-planned and optimum vessel relocation program.

*Keywords: Steel catenary riser, Touch-down zone, Vessel relocation, fatigue damage, fatigue damage spreading, relocation program*

## 1. INTRODUCTION

Steel catenary riser systems are used for the transportation of hydrocarbon production-related materials between the seabed and the host floating platform. Steel catenary risers are the most attractive riser solution because of their simplicity, robustness, and lower procurement costs [1-6]. A major challenge with SCR application is the high stress and fatigue damage incurred around its critical sections, which are the hang off (HO) and the TDZ [5, 7-9], as depicted in Figure 1. The high fatigue response in the SCR HO region is relatively easier to control compared with those occurring at the TDZ. A suitable material of high strength can be employed at the HO region to reduce the high stress and fatigue damage experienced. However, at the touchdown zone, a longer section of the SCR interacts in a complex way with the non-linear seabed, resulting in high and intricate fatigue response patterns that pose great challenges to manage.

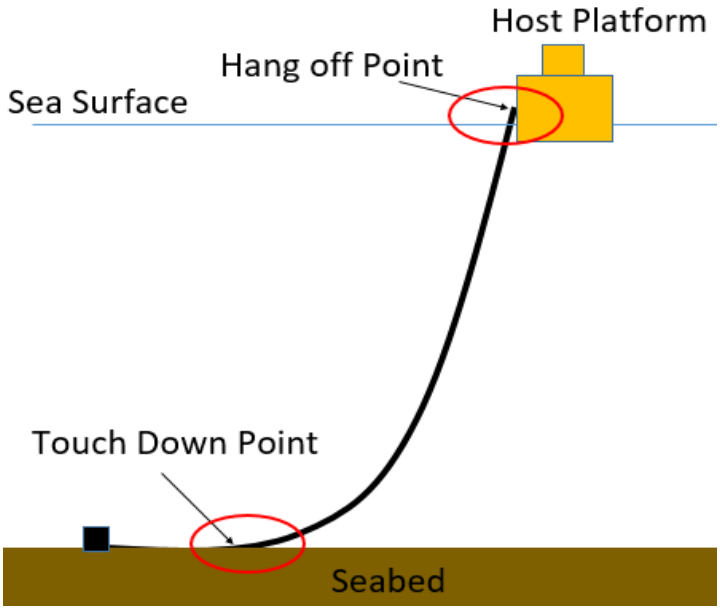


**Figure 1**. Steel catenary riser schematic showing critical sections where stress and fatigue damage responses are higher [10].

Several efforts have been committed by research institutions and the offshore industries to increase the application of SCRs for deepwater hydrocarbon extraction [11-13]. These solutions include the SCR configuration change such as steel lazy wave and shaped riser solutions [14-32], the alternative material application for SCR design such as high strength material including titanium for the riser pipe joint [2, 11, 33-35], the advancement in riser soil interaction modelling such as the development of non-linear riser soil interaction models [36-38], the decoupling of SCR from vessel motion such as the uncoupled steel catenary riser systems [39-42], the vessel relocation to effect fatigue damage spreading along the SCR TDZ [12, 43-45], the use of upset pipe end and titanium welding connection to improve the life of the riser at welded joints [11, 35, 43-50], the use of hydrodynamic dampers which enhances the damping of stress wave propagated from vessel motion to the SCR TDZ [47], etc. The vessel relocation solution for fatigue mitigation in the SCR TDZ has been referenced in literature and have been implemented in real-life projects [12, 43-45]. However, the methodology for investigating and conducting an optimum vessel relocation program is still absent from open literature. This is what this paper is set to present and to demonstrate through an example of a single SCR-vessel system case. The approach presented here can be useful for both new risers and brown field risers for life extension purpose.

The fatigue damage in the active SCR TDZ is proportional to its exposure time to the applied fatigue load, which in turn depends on the variation in the SCR global position and configuration. The relocation of the vessel is a planned variation of the riser host platform from its mean position to effect changes in the global riser configuration, resulting in the spatial (arc length) variation of the SCR fatigue hot spots. The wider the variation or spread of the active seabed section, the higher will be the reduction of the fatigue exposure time and a consequent spread or reduction in the SCR TDZ effective fatigue damage.

To demonstrate this variation, we monitor the offsets of SCR touchdown points (TDPs) by conducting vessel movement in their azimuth direction or riser planes, as shown in Figure 2. Figure 2 (a) presents the SCR TDP offsets from their nominal positions for different SCR configurations with hang-off angles ranging from 8deg to 20deg in a fixed water depth of 1500m, while Figure 2 (b) presents the SCR TDP offset from its nominal position for an SCR

with a hang-off angle of 12deg (with the vertical), in various water depths ranging from 1000m to 3000m. For both scenarios, the vessel offsets are expressed as percentages of the water depths. The negative vessel offsets values are the near vessel offsets where the vessel is relocated towards the SCR TDP along the riser plane. On the other hand, the positive vessel offsets values are for the vessel far offset where the vessel is moved away from the SCR TDP along the riser plane. Note that the vessel in its nominal position (0% offset), incurs no SCR TDP offsets. It could be observed from the plots that the vessel relocation in the far direction imposes larger riser TDP offsets than those of the near vessel offsets. This implies that the SCR TDP horizontal movement is more sensitive to the vessel far offsets. A combination of 10% vessel offsets in both direction for the riser in a water depth of 1500m can be seen to provide more than 200m TDP offset for the SCR with a 12deg hang-off angle (Figure 2 (a)). The TDP offsets are seen to increase with increasing SCR hang-off angle and water depths. For example, it could be observed in Figure 2 (b)) that more than 700m of SCR TDP horizontal travel is possible for an SCR with a 12deg hang-off angle, hosted in a water depth of 3000m, and subjected to 10% vessel offset in the far and near directions. These TDP offsets translate to the spreading of the SCR TDZ fatigue hot spots and a consequent fatigue damage reduction. So, with the relocation program, longer sections of the SCR on seabed share the period of intensive contact with the seabed over the design life of the riser, meaning different fatigue hotspots along the SCR TDZ now receive a reduced number of fatigue load cycles due to the vessel relocation scheme. While the vessel relocation strategy is helpful for brownfield SCRs for life extension purposes [12, 43-45], pre-planning for vessel relocation for a new field development can reduce the stringent requirement for the SCR fatigue design. This can reduce the wall thickness specification, reduce the riser weight and the required design load capacities of the vessel and the hang-off structures and removes the need for SCR TDZ redesign, such as cladded pipe section (e.g. corrosion resistive alloys (CRA)). These potential positive contributions of the vessel relocation technique can significantly reduce the overall cost of the greenfield SCRs.

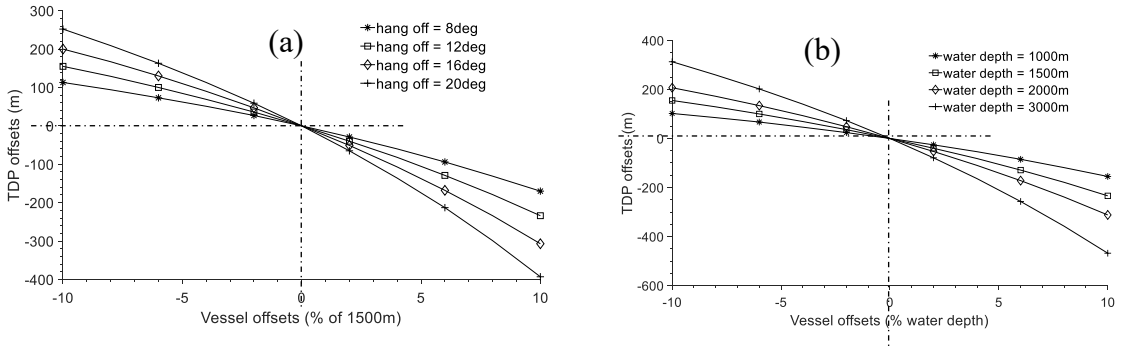


**Figure 2**. SCR touch down point relocation (a) risers with different hang-off angle and different vessel offset conditions in 1500m water depth (b) a 12deg hang off riser in different water depths and different vessel offset conditions.

The planned vessel relocation is a complex operation requiring several inputs, and it is mainly feasible for host platforms with catenary shaped sea keeping systems rather than tension leg platform (TLP). The input to the vessel relocation operation includes but not limited to the directions of the relocation, the number of relocations over the design life of the riser, the number of relocation points or stations, the personnel and equipment required for each relocation operation, the temporary shutdown of production during relocation operation, etc. An appropriate or optimum combination of these variables is required to minimise the fatigue damage of the risers. Concerns may be raised about the optimum vessel relocation direction for a vessel hosting several SCR systems with different azimuth directions. This will be

addressed as an extension of this work in the subsequent investigation, but first, we develop and demonstrate in this paper a method to achieve an optimum vessel relocation for a single SCR.

## 2. VESSEL RELOCATION METHODOLOGY

### 2.1. Definition of terms and SCR TDZ effective fatigue damage

**Vessel relocation program** - All the variables, parameters, activities, and plans involved in the movement of the vessel from one point to another to enhance the spreading of fatigue damage over longer sections of the SCR TDZ are embodied in the *relocation program*. However, in this paper, the relocation program term is used to refer to a unique set of combinations of *the relocation axis,* the *relocation span,* and the *number of relocation stations.* These are the inputs variables for the vessel relocation optimisation analysis in this paper.

**Vessel relocation axis** – From the operational and analysis point of view, it may be relatively easier to conduct a vessel relocation program in a straight line known as the *relocation axis*, as shown in Figure 3. A direction characterises the relocation axis $(\alpha)$ measured from a suitable referenced line. The axis extends from one limit on the riser nearside to the other limit on the riser far side, with the relocation stations equally distributed in between the limits. The optimum relocation axis is one of the design variables for the vessel relocation optimisation problem.

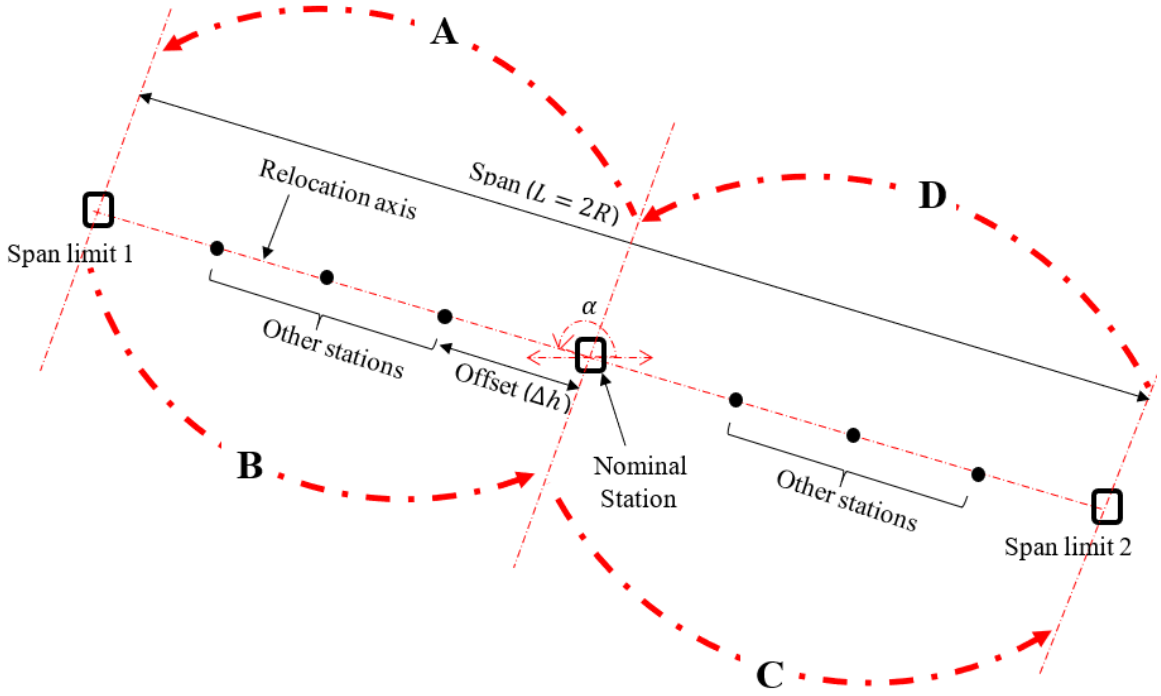


**Figure 3**. A symmetric vessel relocation program layout, depicting equally spaced relocation stations $(p)$ between the relocation span limits $(L)$ along a relocation axis $(\alpha)$.

**Relocation span limits** - The limit on the extent to which the vessel can be moved on either side of the nominal station, along the relocation axis, is constrained by factors including the stress utilisation, the top tension, and the compression around the TDZ of the SCR. The allowable limits within which the relocation program is feasible is referred to as the *span limit, L,* as seen in Figure 3. For the symmetric relocation program considered in this study, the

distance of any of the two-span limits from the nominal station is referred to as the span radius of relocation, $R = L/2$. The span radius is expressed as percentage of the water depth in this study, and it's one of the design variables for the vessel relocation optimisation.

**Relocation stations** - In any relocation program, the vessel is moved intermittently from one position to another, starting from the nominal position (mean or nominal station). These positions are referred to as the *relocation stations,* $p$. For a symmetric vessel relocation program depicted in Figure 3, $p$ will have to be odd, e.g. $p = 3, 5, 7, 9$ etc., as seen in Table 1. For $p = 1$, the vessel is in its nominal station.

**Table 1**. A symmetric vessel relocation program pattern.

| No of stations ($p$) | Station index ($m$) | | | | | | | | | | | | |
|---|---|---|---|---|---|---|---|---|---|---|---|---|---|
| | Nearside | | | | | | Nominal | | | | | | Farside |
| No relocation | | | | | | | 1 | | | | | | |
| 3 | | | | | | 2 | 1 | 3 | | | | | |
| 5 | | | | | 3 | 2 | 1 | 4 | 5 | | | | |
| 7 | | | | 4 | 3 | 2 | 1 | 5 | 6 | 7 | | | |
| 9 | | | 5 | 4 | 3 | 2 | 1 | 6 | 7 | 8 | 9 | | |
| … | | … | … | … | … | … | … | … | … | … | … | … | |
| $k$ | $(k+1)/2$ | ⋯ | 5 | 4 | 3 | 2 | 1 | 6 | 7 | 8 | 9 | ⋯ | $k$ |

**Relocation cycle** - Considering the relocation program in Figure 3, a *relocation cycle* will be the complete movement of the vessel from its nominal station to and from both span limits. The planned journey of the vessel between these span limits involves relocation from one station to another on both sides of the nominal station as indicated by the arrow on A, B, C and D. Each of A, B, C, and D represents a quarter of one relocation cycle and each consist of relocation stations as shown in Figure 3. For example, considering the nine-relocation station program ($p = 9$) in Table 1, one cycle of relocation will consist of the quarter cycles (A, B, C and D) with the following relocation patterns:

$$\text{1 relocation cycle} = \begin{cases} \boldsymbol{A}\text{: } 1 \rightarrow 2 \rightarrow 3 \rightarrow 4 \rightarrow 5. \\ \boldsymbol{B}\text{: } 5 \rightarrow 4 \rightarrow 3 \rightarrow 2 \rightarrow 1 \\ \boldsymbol{C}\text{: } 1 \rightarrow 6 \rightarrow 7 \rightarrow 8 \rightarrow 9 \\ \boldsymbol{D}\text{: } 9 \rightarrow 8 \rightarrow 7 \rightarrow 6 \rightarrow 1 \end{cases} \quad (1)$$

Note that the spread of the fatigue hotspots (fatigue reduction) around the SCR TDZ is related to the time spent at each relocation station and will be independent of the number of relocation cycles. Hence, the methods presented in this paper is based on one relocation cycle.

**Number of relocations** - The number of times the vessel is moved from one station to another is referred to as the *number of relocations* $(n)$. Referring to the 9-station $(p = 9)$ relocation program depicted in equation (1), each quarter of the relocation cycle contains 4 vessel movement. The total number of movements of the vessel for the symmetric 9-station relocation program will be 16. Generally, the number of relocations can be related to the number of relocation station, $p$, as follows:

$$n = 2(p - 1) \quad (2)$$

When $p = 1$ as seen in Table 1, $n = 0$ i.e., no vessel relocation. This is the case representing the traditional approach layout for fatigue analysis where no vessel relocation is considered.

**Relocation offsets** - The direct distance between two neighbouring stations is referred to as the *relocation offset* ($\Delta h$) (see Figure 3). This is the distance over which the vessel is moved during each of the $n$ relocations. For equally spaced relocation stations, the relocation offsets can be obtained from the relocation span, $L$, and the number of relocation stations, $p$, as follows:

$$\Delta h = \frac{L}{p-1} = \frac{2R}{p-1} \tag{3}$$

**Rest and transition time during relocation** - The time spent by the vessel at each of the stations before being moved to a neighbouring station is referred to as the *rest time* ($T_r$). The time it takes to move the vessel from one station to another is referred to as the *transition time* ($T_t$). The following can be observed for the 9-relocation station example from equation (1):

- The nominal station (1) is reached 3 times. This means that the vessel spends a rest time of $3T_r$ at the nominal station.
- Each of the two span limit stations (5 and 9) are reached once. This means the vessel spends a cumulative rest time of $T_r$ each at station 5 and 9.
- The other relocation station ($9-3=2$) are each reached two times. This means that the vessel spends a rest time of $2T_r$ at each of these other $(p-3)$ stations.

This pattern can be generalised for $p$ number of stations ($m = 1$ to $p$) as follows:

$$T_{r_m} = \begin{cases} 3T_r & m = \text{nominal station} \\ T_r & m = \text{span limit1 station} \\ T_r & m = \text{span limit2 station} \\ 2T_r & m = \text{other } (p-3)\text{stations} \end{cases} \tag{4}$$

Where $m$ is the station count ranging from $m = 1$ to $p$, hence, the cumulated rest times across all stations can then be expressed as:

$$T_{r_{cumm}} = \sum_{m=1}^{p} T_{r_m} = 3T_r + T_r + T_r + 2T_r(p-3)$$

$$T_{r_{cumm}} = T_r(2p-1) \tag{5}$$

For $n$ number of relocations, the cumulative transition time will be:

$$T_{t_{cumm}} = nT_t \tag{6}$$

The total exposure time, $T_{cumm}$, can then be expressed as:

$$T_{cumm} = T_{r_{cumm}} + T_{t_{cumm}} = T_r(2p-1) + nT_t \tag{7}$$

The time in transit, $T_t$, is negligible compared with the rest time $T_r$. Operationally, the movement of the vessel from one station to another may take less than a day or a few days, compared with the rest time, which can run into years. Hence, we can rewrite (7) as:

$$T_{cumm} = T_r(2p-1) \tag{8}$$

The total exposure time, $T_{cumm}$ is equal to the design life of the SCR, i.e., $T_{cumm} = T_D$. Hence,

$$T_r = \frac{T_D}{(2p-1)} \tag{9}$$

Substituting equation (9) into equation (4), the resulting coefficient of $T_D$ is expressed in equation (10). This is referred to as the fatigue damage fraction, $f_m$.

$$f_m = \begin{cases} \dfrac{3}{(2p-1)} & m = nominal\ station. \\ \dfrac{1}{(2p-1)} & m = span\ limit1\ station \\ \dfrac{1}{(2p-1)} & m = span\ limit2\ station \\ \dfrac{2}{(2p-1)} & m = other\ (p-3)\ stations \end{cases} \tag{10}$$

Where:

$$\sum_{m=1}^{p} f_m = 1 \tag{11}$$

The resulting (effective) fatigue damage ($D_{eff}$) at any fatigue hotspot in the SCR TDZ for the relocation program can then be expressed as follow:

$$D_{eff} = \sum_{m=1}^{p} f_m D_m \tag{12}$$

Where:

$D_m$ = fatigue damage at station $m$.
$p$ = number of relocation station for the program
$m$ = relocation station counter from 1 to $p$

## 2.2. Fatigue damage for Greenfields and Brownfields

For a new field (greenfield) with an included vessel relocation plan, the fatigue damage of the SCR at the relocation stations, $D_m$, can be obtained considering the design life of the riser $T_D$, appropriate safety factors and other design variables and factors. For example, considering a single occurrence fatigue load case, the Rain flow counting technique [51] can be used to express the varying SCR TDZ stress spectrum as a histogram of stress reversals. The Miner's rule presented in equation (13) can then be applied to cumulate the fatigue damage for the SCR at each of the $m^{th}$ station, where $n_i$ is the number of cycles of the $i^{th}$ stress range components at (station $m$) and $N_i$ is the number of cycles to failure associated with the $i^{th}$ stress range (at station $m$) as obtained from the S-N curve.

$$D_m = \sum_i \frac{n_i}{N_i} \tag{13}$$

For an existing field (brownfield), the objective of the vessel relocation program will be to extend the life of the SCR. Let the remaining or residue fatigue life of the SCR be $T_{rem}$ and the remaining design life of the SCR be $T_{D_{rem}}$. The effective fatigue damage can be calculated using the expressions already presented in equation (12) but with design factors appropriate for existing risers. Also, for brownfield fatigue calculation, $T_D$ will be replaced by $T_{D_{rem}}$ i.e.:

$$T_D = T_{D_{rem}} \tag{14}$$

The life extension, $T_{ext}$, of the SCR can then be obtained as:

$$T_{ext} = \frac{1}{D_{eff}} - T_{rem} \tag{15}$$

## 3. ANALYSIS METHODOLOGY

### 3.1. Vessel relocation optimisation

Each of the relocation programs consists of a unique combination of the axis of relocation ($\alpha$), the span radius ($R = L/2$) and the number of stations ($p$). These are the vessel relocation design variables. A change in any of these variables will result in a different relocation program. Therefore, there is the need to obtain an optimum relocation program that will yield the minimum effective damage $(D_{eff})$ around the SCR TDZ. However, the resulting SCR configuration obtained from any combination of the design variables ($\alpha, R$ and $p$) must satisfy the design limit for the SCR design storm responses. The vessel relocation optimisation problem can, therefore, be cast as follow:

$$\text{find } \mathbf{X} = \begin{Bmatrix} \alpha \\ R \\ p \end{Bmatrix} \text{ which minimises } D_{eff} \tag{16}$$

Subject to the following constraints, **g**:

$$\mathbf{g} = \begin{cases} U_{TDZ} < 1 \\ T_{top} < T_y \\ T_{TDZ} > 0 \end{cases} \tag{17}$$

Where:

$\alpha$ = relocation axis measured from a reference axis.
$R$ = span radius.
$p$ = number of relocation station.
$D_{eff}$ = effective fatigue damage per relocation program.
$U_{TDZ}$ = stress utilisation in the SCR TDZ.
$T_{top}$ = maximum effective tension at the riser top.
$T_{TDZ}$ = minimum effective tension around the riser TDZ.

$T_y$ = yield tension of the riser pipe $= 0.9SA$.
$S$ = Specified minimum yield strength.
$A$ = SCR pipe cross-section area.

Once the design space $(\alpha, R, p)$ is defined for the problem, any suitable optimisation technique can be applied, using the result data obtained for the evaluated objective and constraint functions. In this paper, the index matching optimisation technique is used. Details of the index matching technique are provided in the following section.

### 3.2. Index matching optimisation technique.

Given a general engineering optimisation problem:

$$\text{Minimise: } f(\mathbf{X}) = \begin{Bmatrix} f_1(\mathbf{X}) \\ f_2(\mathbf{X}) \\ . \\ . \\ . \\ f_n(\mathbf{X}) \end{Bmatrix} \tag{18}$$

subject to the following constraints:

$$\mathrm{g_j}(\mathbf{X}) \leq \mathbf{b_j}, \qquad j = 1,2,3 \ldots, r$$

Where:

$$\mathbf{X} = \{\mathbf{x_1}, \mathbf{x_2}, \mathbf{x_3}, \ldots, \mathbf{x_p}\}^{\mathbf{T}}$$

Where:
$f(\boldsymbol{X})$ = a set of objective functions to be optimised.
$\mathrm{g_j}(\mathbf{X})$ = a set of constraint function.
$\mathbf{X}$ = a set of the design variable vectors

The design space can be defined by a unique combination of elements from each vector in **X**. For $k$ such combinations (design points) at which the objective and the constraint functions are evaluated, there will be $k$ elements in each objective function. Let the collection of index vectors, **I**, each containing $k$ indices be assigned to represent the $k$ elements in each of the functions in $f(\mathbf{X})$ as depicted in Figure 4, where **I** is expressed as:

$$\mathbf{I} = \begin{Bmatrix} \boldsymbol{I_1} \\ \boldsymbol{I_2} \\ . \\ . \\ . \\ \boldsymbol{I_n} \end{Bmatrix} \tag{19}$$

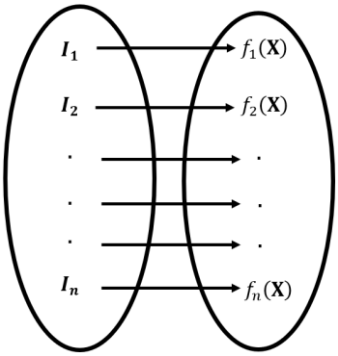


**Figure 4**. Index system of vectors representing elements in each objective function.

The feasible design space, $\mathbf{X_{FDS}}$, is the region where the constraint functions are satisfied. The objective functions' values at the feasible design points can be obtained by evaluating them at $\mathbf{X_{FDS}}$ as shown in equation (20). The corresponding feasible set of index system, $\mathbf{I_{FDS}}$, which is a subset of $\mathbf{I}$ is expressed as shown in equation (21).

$$\mathbf{Y} = \{f(\mathbf{X_{FDS}})\} = \begin{Bmatrix} f_1(\mathbf{X_{FDS}}) \\ f_2(\mathbf{X_{FDS}}) \\ \cdot \\ \cdot \\ \cdot \\ f_n(\mathbf{X_{FDS}}) \end{Bmatrix} \tag{20}$$

$$\mathbf{I_{FDS}} = \{\mathbf{I}(\mathbf{X_{FDS}})\} = \begin{Bmatrix} \boldsymbol{I_1}(\mathbf{X_{FDS}}) \\ \boldsymbol{I_2}(\mathbf{X_{FDS}}) \\ \cdot \\ \cdot \\ \cdot \\ \boldsymbol{I_n}(\mathbf{X_{FDS}}) \end{Bmatrix} \tag{21}$$

If the columns of $\mathbf{Y^T}$ are sorted in ascending order (for minimisation) problem or descending order for maximisation problem, we will have $\mathbf{Y'}$ as presented in equation (22). We can then rearrange elements in the vectors of $\mathbf{I_{FDS}}$ such that their orders match the previous element they represented in vectors of $\mathbf{Y}$ before they were sorted. The re-ordered $\mathbf{I_{FDS}}$ is expressed in equation (23).

$$\mathbf{Y'} = \text{sort}\{\mathbf{Y}^{\mathrm{T}}\} \tag{22}$$

$$\mathbf{I'} = (\mathbf{I_{FDS}})_{\text{reordered}} = \begin{Bmatrix} \boldsymbol{I'_1} \\ \boldsymbol{I'_2} \\ \cdot \\ \cdot \\ \cdot \\ \boldsymbol{I'_n} \end{Bmatrix} \tag{23}$$

The intersection of the indices in the first $q$ rows and across all columns of $(\mathbf{I'})^{\mathbf{T}}$ gives a family of index numbers that represent or point to the sets of optimum design points, i.e.:

$$\mathbf{I_{opt}} = \bigcap_{1}^{q}\{(\mathbf{I}')^{\mathrm{T}}\} \tag{24}$$

The family of optimum design variables, $\mathbf{X_{opt}}$, and the corresponding optimum values of the objective functions, $\mathbf{Y_{opt}}$, can then be obtained through the following matching:

$$\mathbf{X_{opt}} = \mathbf{X}(\mathbf{I_{opt}}) \tag{25}$$

$$\mathbf{Y_{opt}} = \mathbf{Y}(\mathbf{I_{opt}}) \tag{26}$$

The flow chart for the index matching optimisation technique is presented in Figure 5. For a single objective optimisation problem such as the vessel relocation problem in this paper, where the fatigue damage is the objective function, the first index in $\mathbf{I_{opt}}$ points to the best design point or relocation program.

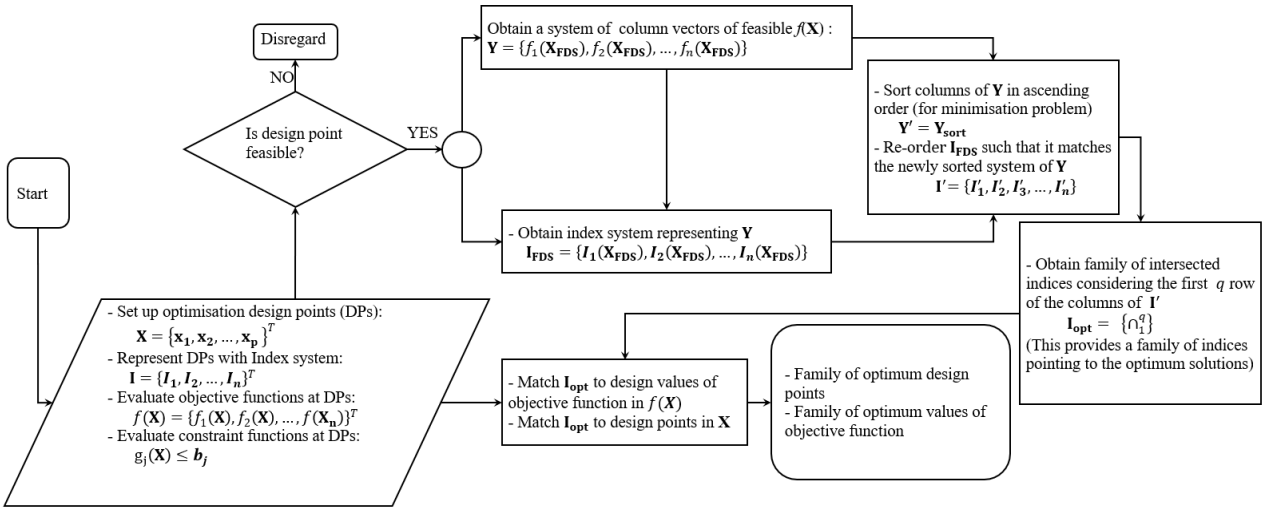


**Figure 5**. Index matching optimisation technique flowchart.

## 3.3. Numerical modelling and analysis

The OrcaFlex numerical software package is used to conduct the analysis for this study. The analysis simulations are performed in the time domain, applying the implicit integration scheme in the numerical solution process. The pre-processing, modelling, simulations and post-processing are automated using MATLAB programs integrated with the OrcaFlex programming interface, OrcFxAPI [52]. The developed MATLAB program pre-processes analysis data and computes additional data required for the numerical modelling in OrcaFlex. The program then generates OrcaFlex models for the relocation programs based on equations developed in this paper. The regular design storm and fatigue wave loads are modelled with the Dean Stream theory, with the wave load acting on the vessel beam to effect maximum roll motions on the SCR.

The storm response analysis is conducted using a single representative regular (design) wave to evaluate the constraint functions. The SCR TDZ stress utilisations, TDZ compressions and top tensions are calculated from the simulated design storm numerical models. The stress utilisation is post-processed using the DNV-OS-F201 combined load (bending, tension, and pressure) resistance factor design criteria. Detailed information about the DNV-OS-F201

criteria can be found in [53]. Similarly, the fatigue analyses for the relocation programs are also conducted using a single regular fatigue wave load to evaluate the SCR TDZ fatigue damage. The objective function (effective fatigue damage, $D_{eff}$) is then post-processed from the SCR TDZ fatigue damage results. For the fatigue calculation, the S-N D-curve in seawater with cathodic protection is used [54]. Once the design storm and effective fatigue damage responses are calculated, the index matching optimisation technique is applied to obtain the indices representing the optimum solutions lying within the shaded region depicted in Figure 6. The applied procedure for the analysis is presented in Figure 7 and summarised as follows:

- Assemble all possible combinations of the design variables ($\alpha$, $R$, $p$).
- Run numerical analyses (for each combination) to determine the values of the constraints ($U, T_{TDZ}, T_{top}$).
- Run numerical analyses (for each combination) to determine the values of the objective function (effective fatigue damage).
- Eliminate combinations that do not satisfy the constraints.
- Order the remaining combinations in ascending order of the objective function to find the combination that minimises the objective function while satisfying the constraints.

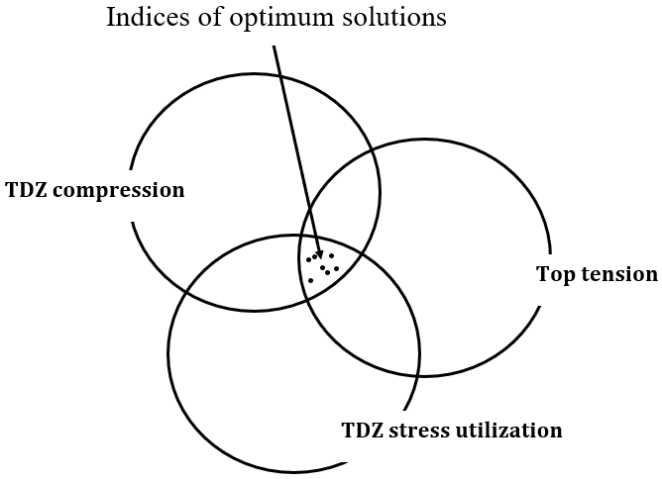


**Figure 6.** Optimum configuration index space.

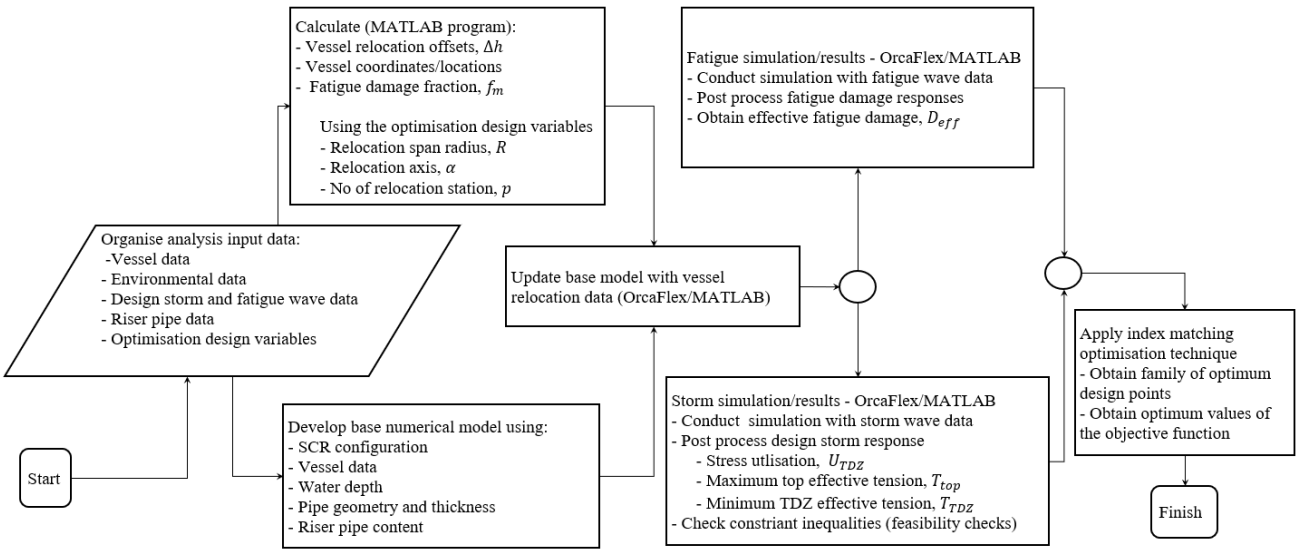


**Figure 7**. Analysis flow chart

# 4. ANALYSIS DATA

## 4.1. Riser pipe data and relocation design variables

The SCR investigated in this work is an 8-inch X70 steel grade pipe hosted by a generic floating production, storage, and offloading (FPSO) unit at an azimuth of 90deg to the vessel heading, as shown in Figure 8. The SCR is connected to the FPSO via a flex joint. The SCR minimum wall thickness required for burst and collapse pressure resistance is calculated based on DNV-OS-F201 criteria [55]. Table 2 presents the analysis data for the study.

**Table 2**. Analysis data.

| SCR data | Values |
|---|---|
| Pipe size | 8inch |
| Internal Design pressure | 10ksi |
| Pipe thickness (fixed) | 16.7mm |
| SMYS | 482 MPa |
| Hang off angle with the vertical | $12^o$ |
| Content density | 600kg/m$^3$ |
| Flex joint stiffness (linear) | 12kN.m/deg |
| Water depth | 1500m |
| S-N curve (seawater plus cathodic protection) | D-Curve [54] |
| Riser design life ($T_D$) (greenfield) | 30 years |
| Relocation axis($\alpha$) | [0,30,60] deg |
| Span radius ($R$)(%water depth) | $\{R{:}1 \leq R \leq 20\}$ |
| Number of station ($p$) | $\{p{:}3 \leq p \leq 19\}$ |

The range of values for the optimisation design variables $(\alpha, R, p)$ presented in Table 2 are briefly discussed as follows:

**Axes of relocation** ($\alpha$) – To cover the full range of relocation directions, six axes are considered. The axes are at 30deg offset from each other and are measured relative to the positive x-axis. As seen in Figure 8, five out of the six axes extend from one side (portside) of the vessel to the other side (starboard), which in this analysis are the SCR nearside and the farside, respectively. The axis-4 aligns with the heading of the vessel. The single SCR system is hosted on the port side and at 90deg to the vessel heading. Since the SCR is perpendicular to the vessel heading, vessel relocation along the axis-4 will cause little variation of the SCR TDZ fatigue hotspots. Hence, axis-4 will not be included in the analysis. The floating production vessel implemented for this study has response amplitude operators (RAOs) that are symmetric about the axis-1 and axis-4. That means, with the SCR orientation, vessel relocation along axis-2 and axis-6 as well as vessel relocation along axis-3 and axis-5 will result in the same response at the SCR TDZ. Hence, vessel relocation along axis-5 and axis-6 will be excluded from the analysis, leaving us with three discrete values of $\alpha$ which are axes-1, axis-2 and axis-3. These axes correspond respectively with 0deg, 30deg, and 60deg measured from the reference axis, as have been presented in Table 2.

**Span radius** ($R$) – Different span radii are considered for the analysis and are expressed as percentages of the water depth. As shown in Table 2, $R$ ranges from 1% to 20% of the water

depth on each of the far and near side of the SCR, i.e., on both side of the nominal station. The span radius is discretised at 1% interval, resulting in 20 discrete values for $R$.

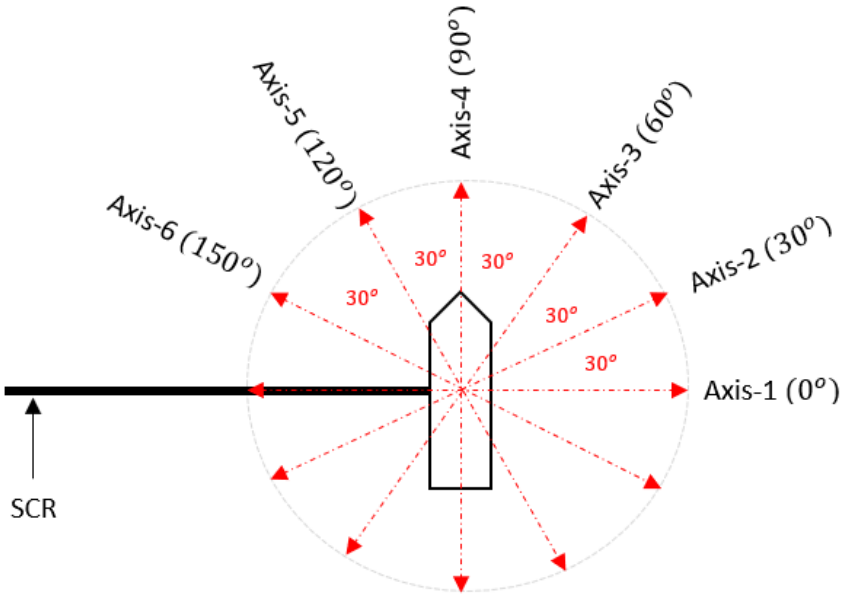


**Figure 8**. The layout of the vessel relocation axes for this study.

**Number of relocation stations ($p$)** – The number of the equally spaced relocation stations along each axis $(\alpha)$ and for each span radius $(R)$ is an odd number, considering a symmetric vessel relocation pattern. As presented in Table 2, the number of stations ranges from 3 to 19 at intervals of 2. This gives 9 discrete values of $p$.

## 4.2. Vessel motion data

A generic response amplitude operator (RAOs) for the FPSO is implemented. Considering the SCR azimuth and connection to the vessel mid-length, the heave and roll RAOs are the most relevant vessel responses to the beam wave acting on the vessel and are presented in Figure 9. The RAOs are symmetrical about the central longitudinal and lateral axes of the FPSO

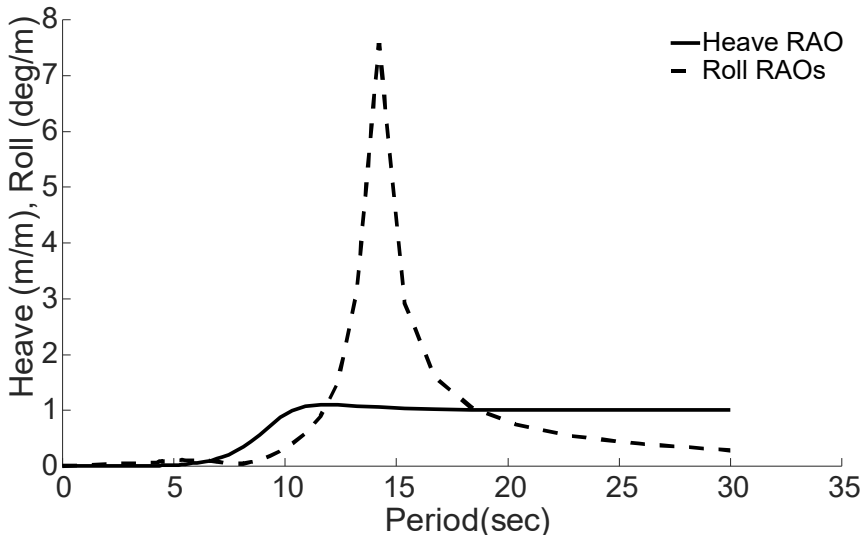


**Figure 9.** Vessel heave and roll RAOs to wave load in the beam sea direction (90deg and 270deg)

### 4.3. Environmental data

The non-linear hysteretic riser soil interaction model detailed in [36] is used in this study. A single regular design storm wave and fatigue sea state are applied during the numerical storm and fatigue analyses. This means the probability of occurrence of the fatigue sea state is 100%. All wave loads are Beam Sea to impact maximum roll motions on the SCR. Both the fatigue and the extreme wave sea state used are presented in Table 3.

**Table 3**. Single wave load data for storm and fatigue analysis

| Analyses | Wave type | Data | Values |
|---|---|---|---|
| Extreme | Regular | $H$ | 8m |
| | | $T$ | 13sec |
| Fatigue | Regular | $H$ | 4.5m |
| | | $T$ | 9.5ec |

The main objective of this study is to develop and demonstrate the vessel relocation methodology. Hence the single wave loads for design storm conditions and fatigue analysis are selected arbitrarily, with periods around the peak of the heave RAO, for demonstration purposes. However, a single representative regular storm and fatigue wave load can be obtained from the irregular wave data available through preliminary screening of the riser hang-off motion at the vessel interface by conducting vessel spectral response calculations [56]. We can use the wave height and associated period causing significant hang-off vertical velocity to represent the design storm wave data. This is reasonable since the SCR vertical hang off velocities correlate with the stress response and compressions of the SCR at the TDZ [57-59] and that different SCR configuration will respond proportionately to different design wave with resulting excitation periods not matching the SCR natural periods. Also, the SCR TDZ fatigue damage correlates with the vertical hang off root mean square (rms) velocity values. With such correlation, a screening of the fatigue wavetable can be conducted to obtain the most effective wave height and associated period that will represent the fatigue wavetable for the optimisation simulations. Note that the single wave data are representative. It will be essential to confirm the performance of the derived optimum riser solution through detailed analysis using the actual storm and the full seastate fatigue wave data.

## 5. ANALYSIS, RESULTS AND DISCUSSION.

Recall from Table 2 that there are 3 discrete values of $\alpha$, and 20 discrete values of $R$. These 2 variables provide 60 $\alpha$-$R$ design points i.e., 2-D design space bordered by $\alpha$ and $R$. Each of these 60 points relates to the 9 discrete values of $p$, with $p$ ranging from 3 to 19 stations at an interval of 2. This gives 540 design points or relocation programs for this study. Now, each of the 540-design points will consist of a varying number of numerical models ranging from $m = 1$ to $p$ as seen in the relocation pattern provided in the annotated Table 4. Hence, the index matching technique index system will have indices ranging from 1 to 540 relocation programs, each containing several models ranging from $m = 1$ to $p$. An alternative way of considering the number of numerical models is to associate the 99 stations in Table 4 to each of the $\alpha$-$R$ 60 design points resulting in 5940 models. Since the storm and the fatigue wave load are different (see Table 3), the number of models simulated for the problems for both the design storm and the fatigue wave load is 11880. For the 540-relocation programs, if any constraint function is not satisfied at any of the $m = 1$ to $p$ station, that relocation program or design point will be deemed infeasible and eliminated from the solution process.

**Table 4**. Vessel relocation patterns

| Number of station ($p$) | Vessel relocation patterns ($m$) | | | | | | | | | | | | | | | | | |
|---|---|---|---|---|---|---|---|---|---|---|---|---|---|---|---|---|---|---|
| 3 | | | | | | | | 2 | 1 | 3 | | | | | | | | |
| 5 | | | | | | | 3 | 2 | 1 | 4 | 5 | | | | | | | |
| 7 | | | | | | 4 | 3 | 2 | 1 | 5 | 6 | 7 | | | | | | |
| 9 | | | | | 5 | 4 | 3 | 2 | 1 | 6 | 7 | 8 | 9 | | | | | |
| 11 | | | | | 6 | 5 | 4 | 3 | 2 | 1 | 7 | 8 | 9 | 10 | 11 | | | |
| 13 | | | | 7 | 6 | 5 | 4 | 3 | 2 | 1 | 8 | 9 | 10 | 11 | 12 | 13 | | |
| 15 | | | 8 | 7 | 6 | 5 | 4 | 3 | 2 | 1 | 9 | 10 | 11 | 12 | 13 | 14 | 15 | |
| 17 | | 9 | 8 | 7 | 6 | 5 | 4 | 3 | 2 | 1 | 10 | 11 | 12 | 13 | 14 | 15 | 16 | 17 |
| 19 | 10 | 9 | 8 | 7 | 6 | 5 | 4 | 3 | 2 | 1 | 11 | 12 | 13 | 14 | 15 | 16 | 17 | 18 | 19 |

**Station ID**

For comparison purposes with the optimum relocation programs, Table 5 presents the TDZ maximum fatigue damage, the stress utilisation, the top effective tension and the TDZ compression for the no-relocation case. For this case, the vessel is kept in the nominal station over the design period, $T_D$. The first 35 members of the feasible optimum relocation programs are presented in Table 6 in their order of performance in terms of $D_{eff}$. The following are data columns reported in the table.

- The index representation of the optimum family members.
- The sets of optimum input design variables $(p, R, \alpha)$ for the optimum design points.
- The effective fatigue damage $(D_{eff})$ in the active SCR TDZ, which is the objective function for the problem.
- The percentage reduction in $D_{eff}$ in the SCR TDZ compared with the no vessel relocation case.
- The maximum stress utilisation $(U_{TDZ})$ in the active SCR TDZ. This is a constraint function on the optimisation problem, which must be less than 1 (see equation (17)).
- The maximum top tension $(T_{top})$ around the SCR hang off region. This is a constraint function whose value must be less than 90% of the yield tension of the riser pipe (see equation (17)).
- The compression in the active SCR TDZ measured as the minimum effective tension $(T_{TDZ})$. This is a constraint function on the optimisation problem, which must be positive, i.e., greater than 0 (see equation (17)). For values less than zero, the riser TDZ is said to be in compression, which is unacceptable during the solution process.

A comparison of the fatigue damage response of the first six optimum relocation programs (index-225, 224, 215, 223, 216, 214) with the no-vessel relocation case is presented in Figure 10. It could be observed for these optimum relocation programs that the $D_{eff}$ are at least 78% lower than the fatigue damage for the no vessel relocation case. This significant reduction is attributed to the effective spreading of the SCR TDZ fatigue hotspot region over a longer riser TDZ section. The redistribution or spreading of the fatigue damage can be seen for each relocation program in Figure 10 compared with the no-relocation case where the fatigue damage is concentrated over a shorter section of the TDZ. It can also be seen that the relocation programs are more effective in reducing the fatigue damage towards the riser anchor rather than towards the riser hang off. The higher reduction in fatigue damage towards the anchor side is caused by the vessel relocation in stations at the riser far side, which causes higher

variation in the active TDZ section than vessel relocations on the riser near side. This SCR TDZ hotspot region variation difference is also demonstrated in Figure 2.

**Table 5**. Fatigue damage and storm responses of SCR for the no-relocation case.

| S/N | Index | $[p, R, \alpha]$ [(-), (%), (deg)] | $D_{eff}$ (/year) | Damage reduction (%) | $U$ | $T_{top}$ (kN) | min $T_{TDZ}$ (kN) |
|---|---|---|---|---|---|---|---|
| 0 | NA | [NA, NA, NA] | 6.0134E-05 | NA | 0.792 | 1532.3 | 12.40 |

**Table 6**. The first 35 members of the optimum relocation programs (design points).

| S/N | Index | $[p, R, \alpha]$ [(-), (%), (deg)] | $D_{eff}$ (/year) | Damage reduction (%) | $U_{TDZ}$ | $T_{top}$ (kN) | min $T_{TDZ}$ (kN) |
|---|---|---|---|---|---|---|---|
| 1 | 225 | [19, 5, 30] | 1.1148E-05 | 81.46 | 0.84 | 1677.74 | 6.15 |
| 2 | 224 | [17, 5, 30] | 1.1306E-05 | 81.20 | 0.84 | 1677.74 | 6.15 |
| 3 | 215 | [17, 4, 30] | 1.1611E-05 | 80.69 | 0.82 | 1645.62 | 7.38 |
| 4 | 223 | [15, 5, 30] | 1.1618E-05 | 80.68 | 0.84 | 1677.74 | 6.15 |
| 5 | 216 | [19, 4, 30] | 1.1619E-05 | 80.68 | 0.82 | 1645.62 | 7.38 |
| 6 | 214 | [15, 4, 30] | 1.1683E-05 | 80.57 | 0.82 | 1645.62 | 7.38 |
| 7 | 36 | [19, 4, 0] | 1.1805E-05 | 80.37 | 0.83 | 1664.32 | 6.65 |
| 8 | 234 | [19, 6, 30] | 1.1897E-05 | 80.22 | 0.84 | 1711.68 | 5.02 |
| 9 | 222 | [13, 5, 30] | 1.1945E-05 | 80.14 | 0.84 | 1677.74 | 6.15 |
| 10 | 35 | [17, 4, 0] | 1.1947E-05 | 80.13 | 0.83 | 1664.32 | 6.65 |
| 11 | 213 | [13, 4, 30] | 1.1977E-05 | 80.08 | 0.82 | 1645.62 | 7.38 |
| 12 | 34 | [15, 4, 0] | 1.2148E-05 | 79.80 | 0.83 | 1664.32 | 6.65 |
| 13 | 45 | [19, 5, 0] | 1.2305E-05 | 79.54 | 0.84 | 1702.33 | 5.35 |
| 14 | 44 | [17, 5,0] | 1.2332E-05 | 79.49 | 0.84 | 1702.33 | 5.35 |
| 15 | 221 | [11, 5, 30] | 1.2395E-05 | 79.39 | 0.84 | 1677.74 | 6.15 |
| 16 | 232 | [15, 6, 30] | 1.2468E-05 | 79.27 | 0.84 | 1711.68 | 5.02 |
| 17 | 233 | [17, 6, 30] | 1.2584E-05 | 79.07 | 0.84 | 1711.68 | 5.02 |
| 18 | 33 | [13, 4, 0] | 1.2587E-05 | 79.07 | 0.83 | 1664.32 | 6.65 |
| 19 | 43 | [15, 5, 0] | 1.2633E-05 | 78.99 | 0.84 | 1702.33 | 5.35 |
| 20 | 25 | [15, 3, 0] | 1.2669E-05 | 78.93 | 0.82 | 1628.42 | 8.01 |
| 21 | 27 | [19,3,0] | 1.2671E-05 | 78.93 | 0.82 | 1628.42 | 8.01 |
| 22 | 212 | [11, 4, 30] | 1.2743E-05 | 78.81 | 0.82 | 1645.62 | 7.38 |
| 23 | 243 | [19, 7, 30] | 1.2751E-05 | 78.80 | 0.85 | 1747.49 | 4.01 |
| 24 | 26 | [17, 3, 0] | 1.2755E-05 | 78.79 | 0.82 | 1628.42 | 8.01 |
| 25 | 441 | [19, 9, 0] | 1.2834E-05 | 78.66 | 0.83 | 1693.05 | 6.52 |
| 26 | 24 | [13, 3, 0] | 1.2861E-05 | 78.61 | 0.82 | 1628.42 | 8.01 |
| 27 | 54 | [19, 6, 0] | 1.2864E-05 | 78.61 | 0.85 | 1742.42 | 4.16 |
| 28 | 431 | [17, 8, 0] | 1.2971E-05 | 78.43 | 0.83 | 1672.23 | 6.98 |
| 29 | 432 | [19, 8, 0] | 1.2979E-05 | 78.42 | 0.83 | 1672.23 | 6.98 |
| 30 | 242 | [17, 7, 30] | 1.3034E-05 | 78.33 | 0.85 | 1747.49 | 4.01 |
| 31 | 231 | [13, 6, 30] | 1.3042E-05 | 78.31 | 0.84 | 1711.68 | 5.02 |
| 32 | 422 | [17, 7, 0] | 1.3083E-05 | 78.24 | 0.82 | 1651.90 | 7.50 |
| 33 | 421 | [15, 7, 0] | 1.3115E-05 | 78.19 | 0.82 | 1651.90 | 7.50 |
| 34 | 32 | [11, 4, 0] | 1.3120E-05 | 78.18 | 0.83 | 1664.32 | 6.65 |
| 35 | 211 | [9, 4, 30] | 1.3163E-05 | 78.11 | 0.82 | 1645.62 | 7.38 |

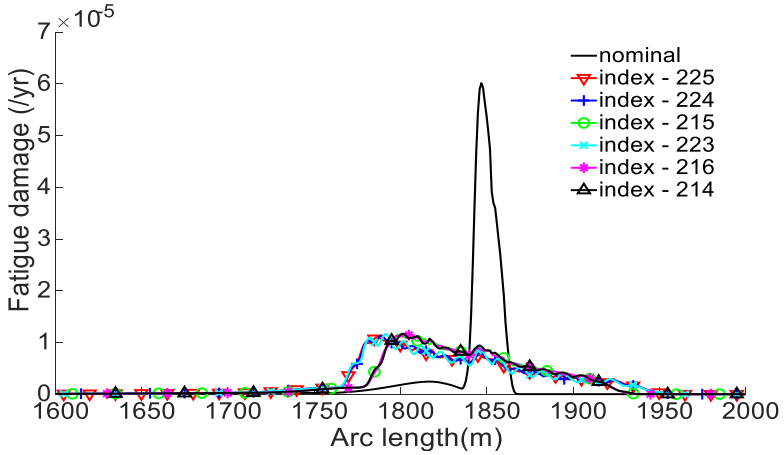


**Figure 10.** Effective fatigue damage for the first 6 optimum relocation programs compared with the no-relocation case where the vessel is kept in the nominal station over the SCR design life.

From the analysis result in Table 6, it is observed that the best relocation program (index-225) is not necessarily along the riser plane axis ($\alpha = 0$deg) as is generally expected, but along the ($\alpha = 30$deg) axis. However, a relocation program along the riser plane axis (index-36) also provided a significant improvement in the fatigue damage response. It appeared as the seventh-best relocation program with 80.37% fatigue damage reduction. Index-225 and index-36 are similar in terms of the number of station ($p$ =19) but different in terms of the span radius ($R =$ 5% and 4% respectively), and relocation axis ($\alpha = 0$deg and 30deg respectively). To compare the relocation programs for these different $R$ and $\alpha$, the $D_{eff}$ range graph maximum is plotted in Figure 11 (a) for index 45, index-225 and index-405 ($p = 19, R = 5\%$, $\alpha = 0$deg, 30deg and 60deg respectively), and index-36, index-216 and index-396 ($p = 19, R = 4\%, \alpha = 0$deg, 30deg and 60deg respectively). The maximum values of the $D_{eff}$ are presented in Figure 11 (b). Here, the $D_{eff}$ along the 30deg axis for $R = 4\%$ and $R = 5\%$ are lower than $D_{eff}$ along 0deg.

To explore why the relocation program along other axes could have higher performance than relocation along the SCR plane axis, a three-station vessel relocation program is considered, with 5% vessel offset from the mean station. Instead of the three-axis (0deg, 30deg and 60deg) considered during the optimisation solution process, we conduct the vessel relocation analysis along 180 directions ranging from 2deg to 358deg at 2deg interval. The maximum fatigue damage around the SCR TDZ at each station (apart from the mean station) along each relocation axis follows the behaviour presented in Figure 12(a). The figure shows that the most significant fatigue damage is experienced when the vessel is relocated towards the SCR TDZ (near-near offset, 180deg), causing higher fluctuating bending stress response and more significant TDZ fatigue damage. However, when the vessel is relocated in the direct opposite direction (far-far offset, 0deg), the fatigue damage is minimum, resulting from the stretching and associated reduced fluctuating bending stress around the TDZ. Since the relocation station in both directions of any axis plus the nominal station makes up the number of station ($p = 3$) along that axis, the effective damage, $D_{eff}$, will be a sum of the stations' fatigue damages factored by their damage fractions. Similar consideration can be made for all axes consisting of vessel offset in both directions, as shown in Figure 12(b). It is evident from Figure 12(b) that there will be some axes of relocation that provide reduced $D_{eff}$ than the axis coinciding with the riser plane ($\alpha = 0$deg/180deg). This indicates that the optimum relocation program may not be along the riser plane. Extending the same for the optimum case in this study (index-225, see Table 6), with a higher number of stations ($p$ =19), similar findings are applicable.

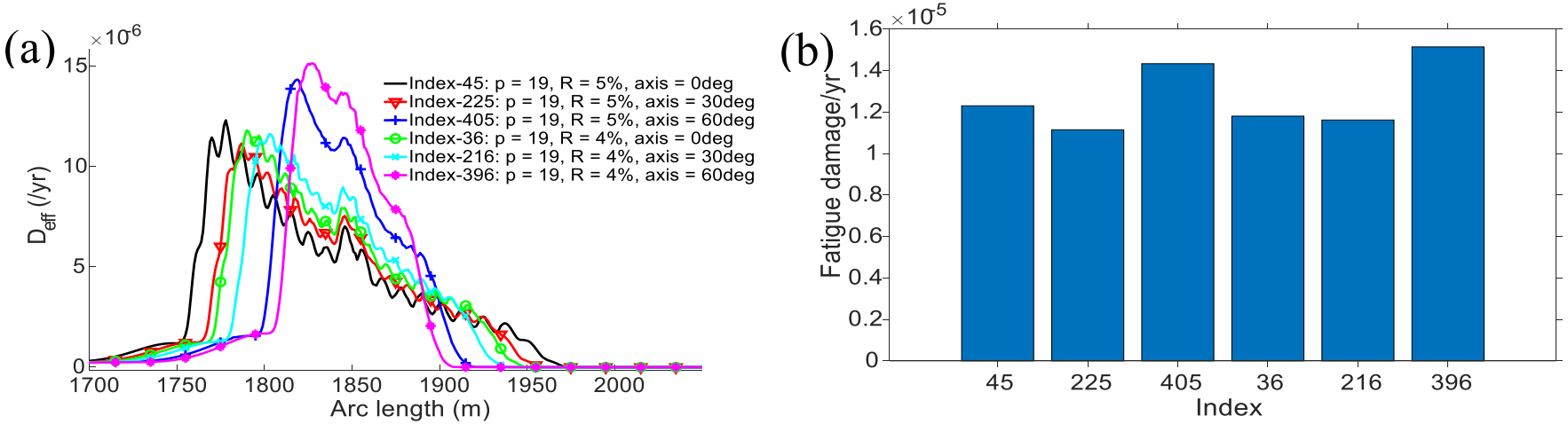


**Figure 11.** (a) $D_{eff}$ range graph maximum for relocation program along the three axes for $(p = 19, R = 5\%, R = 4\%)$, (b) Maximum $D_{eff}$ for relocation program along the three axes for $(p = 19, R = 5\%, R = 4\%)$,

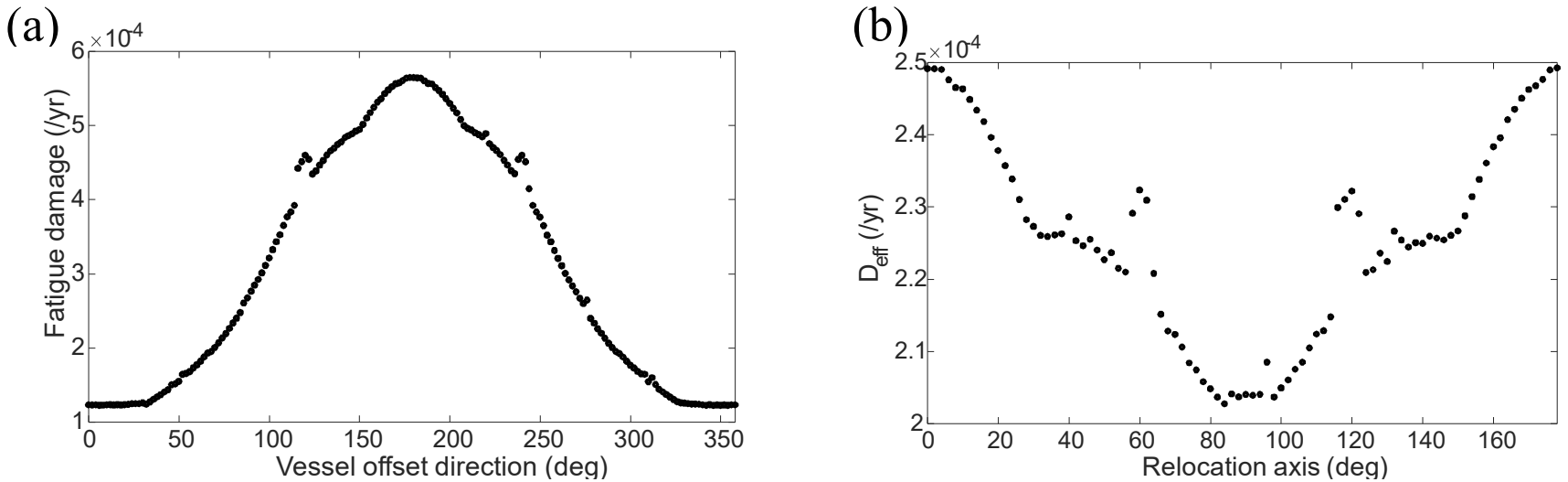


**Figure 12.** Maximum SCR TDZ fatigue damage response for 3-station relocation program ($p = 3$) with vessel offset of 5% (from nominal station) in all direction, (b) Resulting maximum effective fatigue damage for the 3-station relocation program ($p = 3$) with vessel 5% along all axes.

Revisiting Table 6, it can also be observed that the improvement in fatigue damage response increases with increasing $p$. For a given $p$, the fatigue exposure time over the design life ($T_D$) does not (in general) change with respect to $\alpha$ and $R$. However, $\alpha$ and $R$ affect the configuration of the SCR, which in turn influence the configuration of the fatigue hotspots and a consequential impact on the fatigue damage. Larger $R$ will result in higher TDZ fluctuating bending moments for stations in the riser near directions, causing more significant fatigue damage. It can be observed from Table 6 that the first 22 best relocation programs are limited to about $R = 6\%$ of the water depth. Relocation programs with higher values of $R$ such as index-243 ($R = 7\%$ of water depth) and index - 441 ($R = 9\%$ of water depth) perform less than the best six relocation programs. However, it is noted that their performances are still significantly higher than those of the SCR for the no-relocation case. For even higher values of $R$, the fatigue performances for the corresponding relocation programs decreases and are located down the performance list or removed from the solution process for violation of the constraint functions (especially the $U_{TDZ}$ and $T_{TDZ}$).

## 5.1. Constraint function responses

The index matching technique retains the relocation programs which satisfy the constraint function, as seen in the constraint function columns in Table 6. All the values of the three-constraint functions ($U_{TDZ}$, $T_{top}$ and $T_{TDZ}$) for the optimum relocation programs are within the constraint's limits (see equation (17)). The order of performance of the SCR response to the design storm wave condition does not necessarily have to be in the order of fatigue performance if the constraint inequalities are satisfied. Updating any of the constraint limits in equation (17) will result in new sets of optimum relocation programs. For example, if it should be considered that the SCR TDZ minimum tension (compression) must be greater than 8kN, then the best relocation program becomes index-25, while others before and after it that do not satisfy this new constraint are eliminated. This indicates how sensitive the relocation program is to the constraint functions imposed by the SCR storm responses and the designer's choice. The index matching technique can capture these changes when constraint functions are updated without the need to rerun the simulations.

The range graph maximum of the stress utilisation ($U_{TDZ}$) for the first six best relocation programs from Table 6 and that of the no-relocation case are presented in Figure 13. Note that these response profiles connect the nodal maximum across the stations ($m = 1$ to $p$) for each relocation program, with an observable spread of higher $U_{TDZ}$ over longer section of the SCR TDZ. However, for the no-relocation case, the riser range graph is maximum within short sections of the TDZ since the SCR remains in the nominal station (station-1) all through its design life. It is observed from Figure 13 for the six optimum programs that the stress utilisation resulting from the combined load can be higher than that of the no-relocation case, especially in the TDZ section towards the vessel. Higher $U_{TDZ}$ occur during vessel positions in stations on the near side of the riser, as these impose higher bending stress around the TDZ, hence higher $U_{TDZ}$ than that of the no-relocation case. Index-215, 216 and 214 relocation programs with $R = 4\%$ have equal $U_{TDZ}$ although they have different $p$. Similarly, equal $U_{TDZ}$ is observed for index-225, 224 and 223 relocation programs with $R = 5\%$. As expected, $U_{TDZ}$ increases with increasing $R$ as the vessel is relocated towards the SCR anchor as observed with relocation programs with $R = 5\%$ compared with relocation programs with $R = 4\%$.

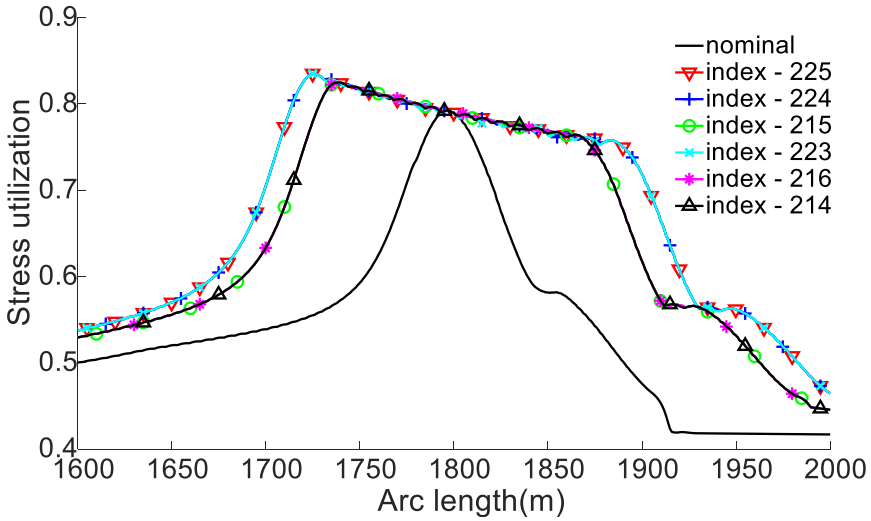


**Figure 13.** Maximum stress utilisation in the active SCR TDZ across the stations for the best 6 relocation programs.

The range graph maximum of the second constraint function ($T_{top}$) for the first six best relocation programs from Table 6 and that of the no-relocation case is presented in Figure 14. Again, it should be noted that these values are the maximum across the relocation stations contained in each of the relocation programs, except that of the no-relocation case where the riser remains in nominal position throughout the design life. All the six best relocation programs give maximum tension around SCR hang off that is higher than that of the no-relocation case but are, however, below 90% of the yield tension (see equation (17)). Higher top tension than the no-relocation case occurs when the vessel is in stations on the far side of the SCR. This results in a more extended hanging riser section and a consequent increased in top tension. Index-215, 216 and 214 relocation programs have equal maximum top tension as should be expected since their span radii ($R = 4\%$) are equal, although they contain different stations ($p$), which are 17 19, 15, respectively. Similar behavior is seen for the top tension of index-225, 224 and 223 relocation programs, where they possess the same $R$ value of 5%. The relocation programs with $R$ = 5% are expected to have higher top tension than those with $R = 4\%$ as observed from Figure 14. This is because farther vessel position from the nominal station in the riser far direction causes a longer hanging riser section resulting in higher top tension.

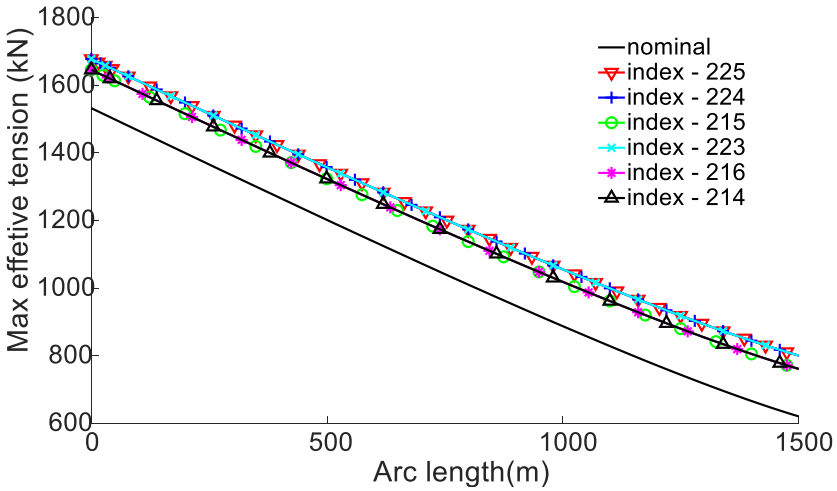


**Figure 14.** Maximum effective tension in the SCR hang-off region across the relocation stations for the best 6 relocation program.

The range graph minimum of the third constraint function ($T_{TDZ}$) for the first six best relocation programs from Table 6 and that of the no-relocation case are presented in Figure 15. Like the SCR TDZ stress utilisation, we expect higher compression in the active TDZ for these six relocation programs when compared with the no-relocation case. This is because the SCR experiences higher compression around the TDZ when the vessel occupies stations on the nearside of the riser. The TDZ compression response for index-215, 216 and 214 relocation programs have a common span radius, $R = 4\%$, and hence same TDZ compression responses. A similar behaviour is observed for index-225, 224 and 223 relocation programs with $R = 5\%$. For the same reason given for $U_{TDZ}$, considering equal number of stations $p$, the compression for relocation programs with $R = 5\%$ will be (slightly) higher than those with $R = 4\%$ as can be seen from Table 6 and Figure 15.

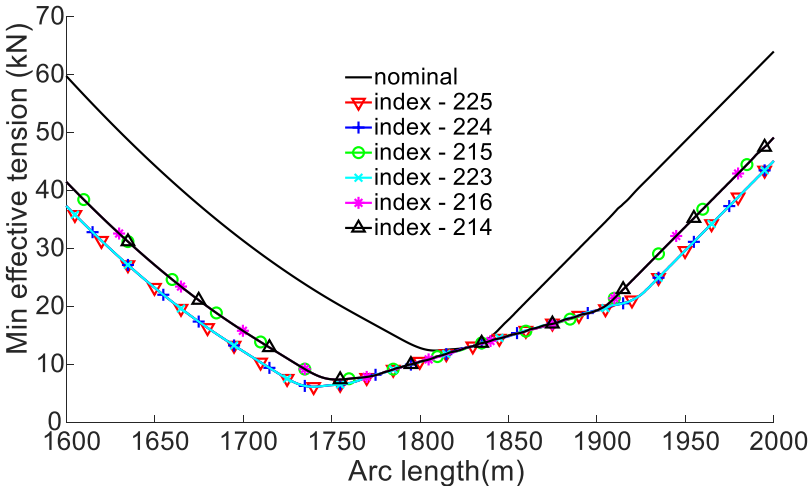


**Figure 15.** Maximum compression (minimum effective tension) in the active SCR TDZ across the stations in the best 6 relocation programs.

## 5.2. A detailed discussion of the Index-225 relocation program.

The index-225 represents the best relocation program for the vessel relocation optimisation analyses in this paper. A detailed consideration of this first and best optimum program (the first row in Table 6 shows that there are $p = 19$ equally spaced stations, with relocations limited to a span radius, $R = 5\%$ of the water depth in both the far and the near direction of the SCR. This means that to satisfy the constraint functions and obtain minimum fatigue damage, the vessel movement is limited within 75m (5% ×1500m), each in the far and the near direction along the axis, $\alpha = 30$deg. This gives a relocation span ($L = 2R$) of 150m. The relocation offset ($\Delta h$), i.e., the distance between two neighbouring stations is 8.33m, obtained using equation (3) and the number of times ($n$) that the vessel is relocated over the SCR design life $T_D$, is 36 times, obtained using equation (2). For the $p$ =19 stations in this relocation program, the cumulative exposure time over the SCR design life ($T_D$ =30yrs.) at each station will follow the pattern depicted by the damage fraction ($f_m$) presented in Figure 16. It should be recalled that the exposure time is $T_D$ factored by $f_m$, where the $f_m$ at each of the stations ($m = 1\ to\ p$) are calculated from equation (10). The exposure times at each of the 19 stations are presented in Table 7. The unfactored fatigue damage responses of the active SCR TDZ at each of the 19 stations are shown in Figure 17, and the corresponding constraint function responses ($U_{TDZ}, T_{top}, T_{TDZ}$) at each of the 19 stations are presented in Figure 18, Figure 19 and Figure 20, respectively.

**Table 7**. Fatigue damage fraction ($f_m$) and exposure time ($T_{rm}$) for the 19 stations of the index-225 relocation program over the SCR design life ($T_D$) of 30yrs.

| Station ID ($m =$) | Station Description | Damage fraction | Exposure Time (yrs.) |
|---|---|---|---|
| 1 | Nominal | 0.081 | 2.43 |
| 10 | Span limit1 | 0.027 | 0.81 |
| 19 | Span limit2 | 0.027 | 0.81 |
| Others | $(p-3)$ stations | 0.054 | 1.62 |

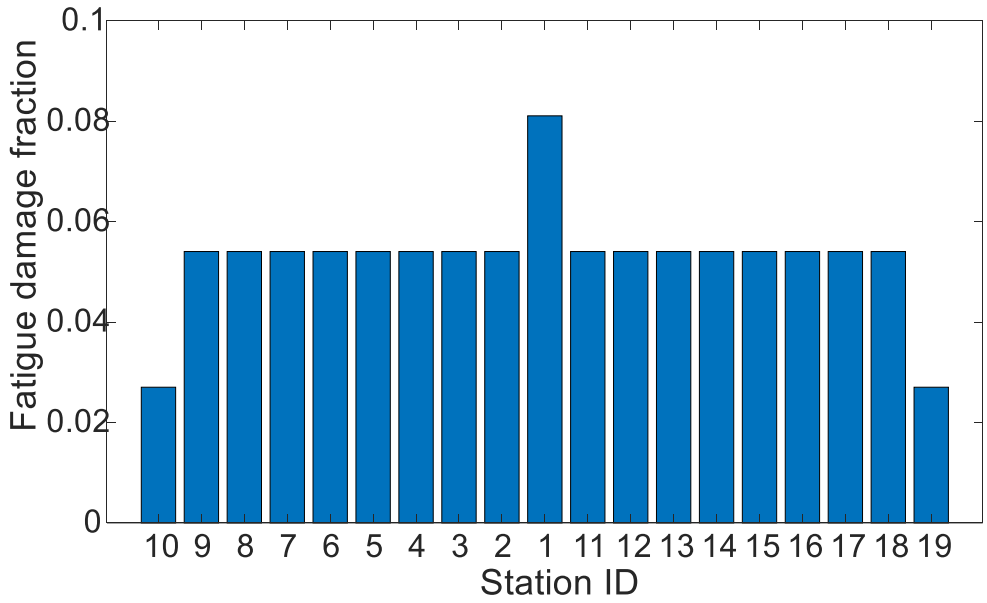


**Figure 16.** Fatigue damage fraction for the 19 relocation stations in the index-225 vessel relocation program.

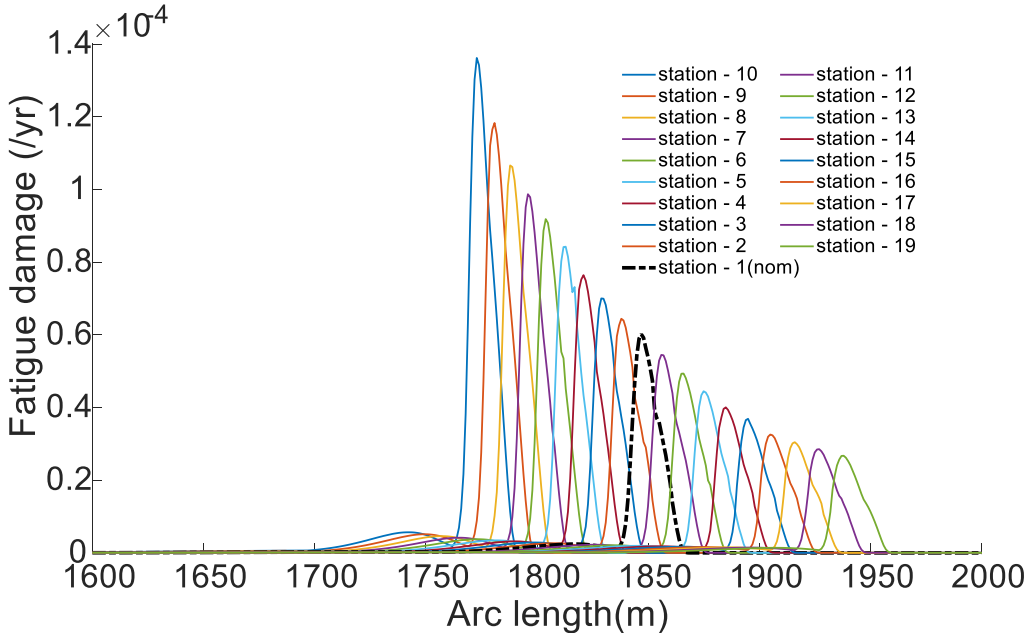


**Figure 17.** SCR TDZ fatigue damage at the 19 stations for index-225 relocation program: $p = 19, \alpha = 30^o, R = 5\%$

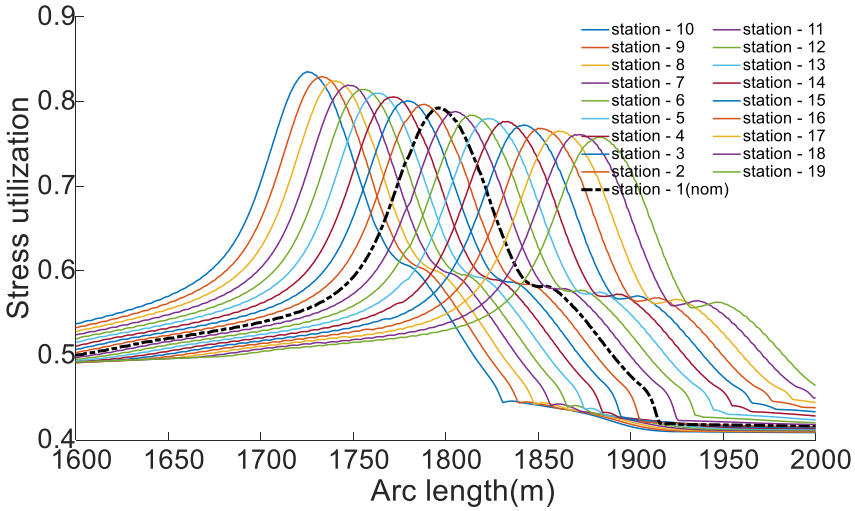


**Figure 18.** SCR TDZ stress utilisation at the 19 stations for index-225 relocation program: $p = 19, \alpha = 30^o, R = 5\%$

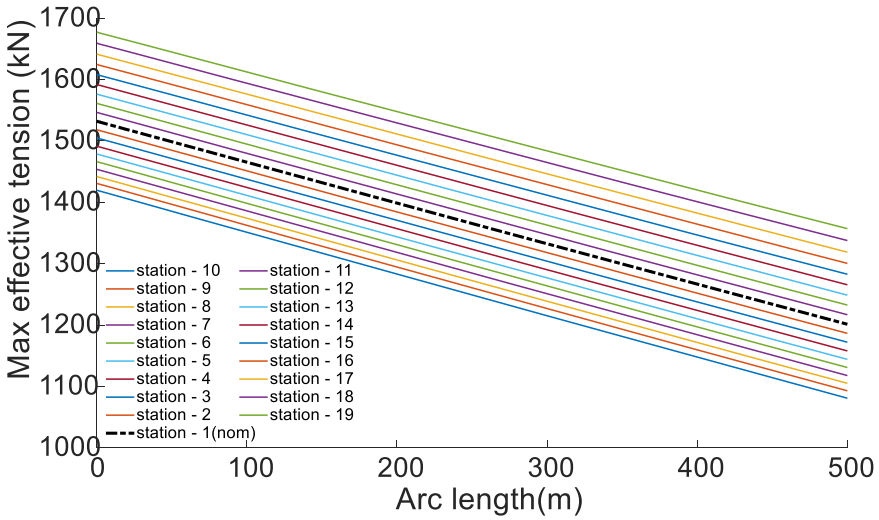


**Figure 19.** SCR maximum top tension at the 19 stations for index-225 relocation program: $p = 19, \alpha = 30^o, R = 5\%$

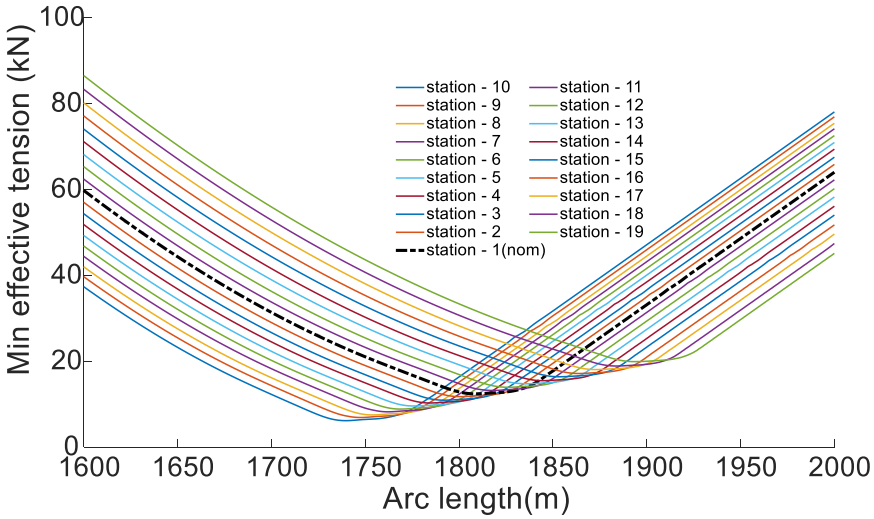


**Figure 20.** SCR TDZ compression (min. effective tension) at the 19 stations for index-225 relocation program: $p = 19, \alpha = 30^o R = 5\%$

It could be seen from Figure 17 that the highest of the maximum fatigue damage occur at station-10, which is the span limit station on the SCR near side (towards seabed anchor). The vessel position in station-10 causes significant global compression and higher fluctuating bending moments in the SCR TDZ compared with configurations at other relocation stations. This result in a higher fatigue damage response, as seen in Figure 17. The reverse is the case for station-19, where the SCR global configuration is stretched, and less fluctuating bending occurs at the TDZ resulting in minimum fatigue damage compared with other stations. The vessel in station-1 (nominal station) imposes fatigue damage of magnitude between the above extreme configuration conditions.

The effectiveness of any vessel relocation program is measured by its ability to level out the peakedness of the fatigue damage response in the active SCR TDZ, i.e., the capacity to impose a wider spread of the fatigue hotspot region. It could be seen from Figure 17 that the fatigue damage is concentrated within short regions of the SCR TDZ with the vessel in each of the 19 stations. Table 8 presents the maximum fatigue damage responses and the arc length where they occur within the active SCR TDZ for the 19 stations in the index-225 relocation program. The leading diagonal terms are the maximum fatigue damage at the respective 19 stations, with the corresponding critical arc lengths in the first column of the table. The off-diagonal terms are the associated damages occurring at other stations' critical arc lengths. For example, the critical damage arc length when the vessel is at station-1 is 1846.8m, and the critical damage arc length when the vessel is at station-19 is 1937.8m. When the vessel is at station-1, the fatigue damage at arc length 1937.8m is about 60000 times smaller than the fatigue damage at arclength 1846.8m. On the other hand, at station-19, the fatigue damage at arc length 1846.8m is about 115 times smaller than the fatigue damage at arclength 1937.8m. The maximum fatigue damage when the vessel is at stations 1 and 19, with the associated fatigue damage occurring at other stations' critical arc lengths, are presented in Figure 21 and Figure 22, respectively.

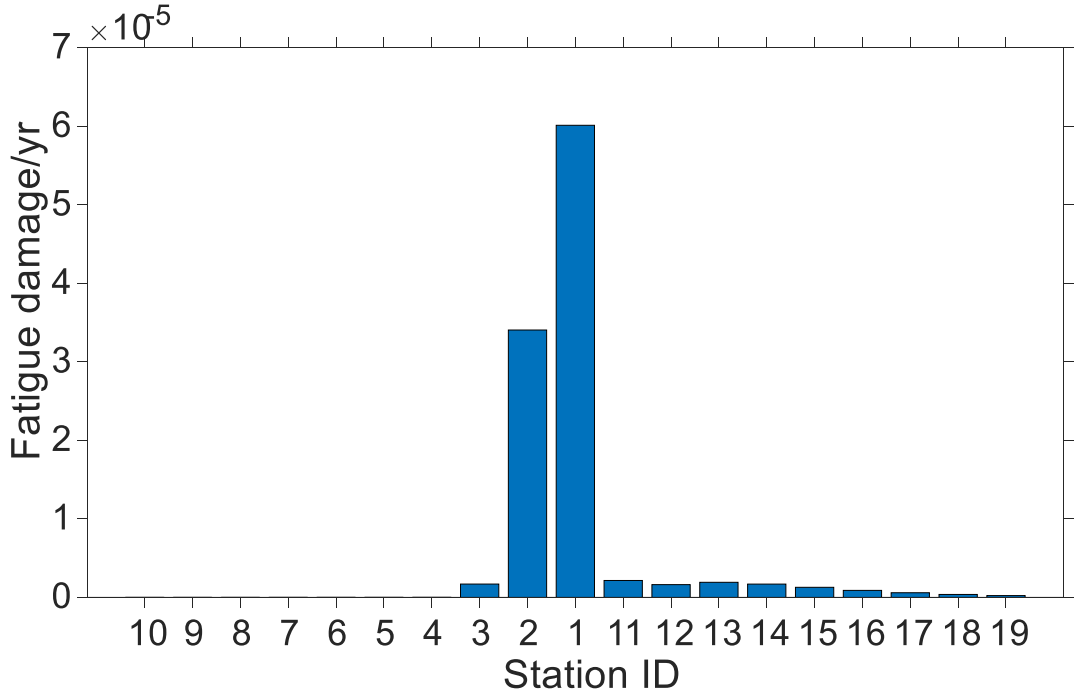


**Figure 21.** Fatigue damage at station-1 with the associated fatigue damage at other stations' critical arc lengths

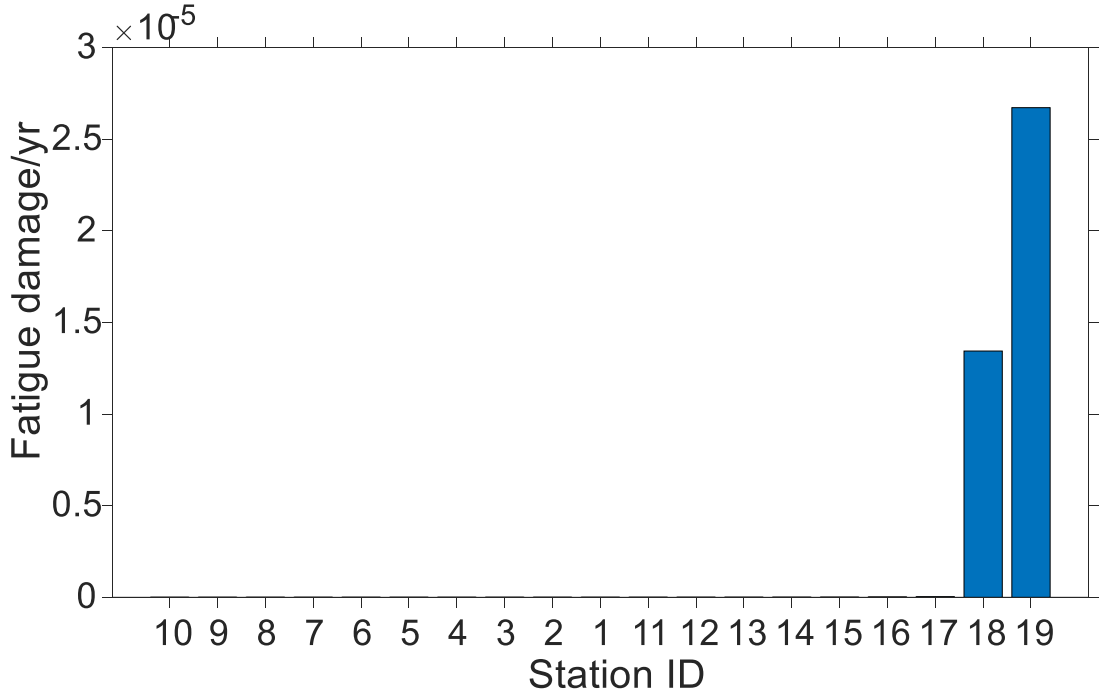


**Figure 22.** Fatigue damage at station-19 with the associated fatigue damage at other stations' critical arc lengths

**Table 8**. Fatigue damage in SCR TDZ at the 19 relocation stations for index - 225 relocation program: Shaded diagonal terms are the maximum damage, and the corresponding arc length is the point the maximum damage occurs; The off-diagonal terms are the associated damage at other arc lengths where the critical damages occur for other relocation stations.

**Relocation stations**

| Arc lengths (m) | 10 | 9 | 8 | 7 | 6 | 5 | 4 | 3 | 2 | 1 | 11 | 12 | 13 | 14 | 15 | 16 | 17 | 18 | 19 |
|---|---|---|---|---|---|---|---|---|---|---|---|---|---|---|---|---|---|---|---|
| 1772.846 | 136.173 | 8.788 | 2.411 | 3.650 | 3.757 | 3.106 | 2.187 | 1.425 | 0.867 | 0.505 | 0.279 | 0.186 | 0.178 | 0.173 | 0.178 | 0.182 | 0.182 | 0.181 | 0.190 |
| 1780.846 | 72.864 | 118.278 | 10.178 | 2.154 | 3.302 | 3.436 | 2.805 | 1.991 | 1.287 | 0.791 | 0.458 | 0.256 | 0.167 | 0.162 | 0.170 | 0.175 | 0.180 | 0.179 | 0.187 |
| 1787.846 | 11.376 | 68.971 | 106.601 | 5.633 | 2.239 | 3.199 | 3.145 | 2.474 | 1.717 | 1.116 | 0.680 | 0.396 | 0.214 | 0.152 | 0.159 | 0.168 | 0.174 | 0.175 | 0.182 |
| 1795.846 | 0.012 | 8.158 | 59.995 | 98.685 | 5.331 | 2.078 | 2.945 | 2.834 | 2.216 | 1.554 | 1.006 | 0.615 | 0.351 | 0.195 | 0.145 | 0.158 | 0.165 | 0.168 | 0.174 |
| 1803.846 | 0.014 | 0.012 | 6.495 | 53.551 | 91.839 | 4.609 | 2.006 | 2.731 | 2.597 | 2.002 | 1.398 | 0.904 | 0.547 | 0.318 | 0.177 | 0.144 | 0.153 | 0.160 | 0.164 |
| 1812.846 | 0.006 | 0.010 | 0.012 | 2.574 | 45.209 | 84.236 | 6.230 | 1.823 | 2.516 | 2.378 | 1.854 | 1.294 | 0.843 | 0.519 | 0.305 | 0.171 | 0.138 | 0.146 | 0.152 |
| 1820.846 | 0.006 | 0.005 | 0.008 | 0.011 | 2.865 | 43.398 | 76.413 | 4.318 | 1.805 | 2.353 | 2.169 | 1.675 | 1.160 | 0.758 | 0.465 | 0.272 | 0.160 | 0.132 | 0.141 |
| 1828.846 | 0.003 | 0.006 | 0.005 | 0.006 | 0.009 | 3.600 | 42.310 | 70.013 | 2.645 | 1.793 | 2.218 | 1.989 | 1.510 | 1.043 | 0.678 | 0.413 | 0.253 | 0.147 | 0.128 |
| 1837.846 | 0.001 | 0.002 | 0.004 | 0.006 | 0.005 | 0.008 | 2.316 | 37.423 | 64.420 | 2.550 | 1.693 | 2.067 | 1.838 | 1.391 | 0.967 | 0.627 | 0.400 | 0.242 | 0.144 |
| 1846.846 | 0.001 | 0.001 | 0.001 | 0.002 | 0.004 | 0.004 | 0.006 | 1.700 | 34.059 | 60.134 | 2.156 | 1.628 | 1.924 | 1.696 | 1.286 | 0.894 | 0.595 | 0.376 | 0.232 |
| 1855.846 | 0.001 | 0.001 | 0.001 | 0.002 | 0.002 | 0.003 | 0.003 | 0.005 | 1.530 | 32.987 | 54.477 | 1.652 | 1.573 | 1.828 | 1.569 | 1.198 | 0.835 | 0.552 | 0.354 |
| 1865.846 | 0.001 | 0.001 | 0.001 | 0.001 | 0.001 | 0.002 | 0.003 | 0.003 | 0.004 | 0.520 | 27.936 | 49.346 | 1.863 | 1.465 | 1.710 | 1.492 | 1.128 | 0.799 | 0.537 |
| 1874.846 | 0.000 | 0.001 | 0.001 | 0.001 | 0.001 | 0.002 | 0.002 | 0.003 | 0.003 | 0.004 | 0.828 | 26.623 | 44.468 | 1.054 | 1.462 | 1.607 | 1.374 | 1.049 | 0.742 |
| 1884.846 | 0.000 | 0.001 | 0.001 | 0.001 | 0.001 | 0.001 | 0.002 | 0.002 | 0.003 | 0.003 | 0.005 | 0.446 | 23.188 | 40.037 | 0.978 | 1.383 | 1.537 | 1.311 | 0.995 |
| 1894.846 | 0.000 | 0.000 | 0.001 | 0.001 | 0.001 | 0.001 | 0.001 | 0.002 | 0.002 | 0.003 | 0.004 | 0.006 | 0.308 | 20.706 | 36.886 | 0.851 | 1.349 | 1.465 | 1.239 |
| 1904.846 | 0.000 | 0.000 | 0.000 | 0.001 | 0.001 | 0.001 | 0.001 | 0.002 | 0.002 | 0.002 | 0.003 | 0.005 | 0.009 | 0.259 | 18.600 | 32.565 | 0.792 | 1.311 | 1.394 |
| 1915.846 | 0.000 | 0.000 | 0.000 | 0.001 | 0.001 | 0.001 | 0.001 | 0.001 | 0.002 | 0.002 | 0.003 | 0.004 | 0.005 | 0.012 | 0.083 | 16.569 | 30.461 | 0.762 | 1.268 |
| 1926.846 | 0.000 | 0.000 | 0.000 | 0.000 | 0.001 | 0.001 | 0.001 | 0.001 | 0.001 | 0.002 | 0.002 | 0.003 | 0.004 | 0.006 | 0.014 | 0.039 | 15.141 | 28.534 | 0.756 |
| 1937.846 | 0.000 | 0.000 | 0.000 | 0.000 | 0.000 | 0.001 | 0.001 | 0.001 | 0.001 | 0.001 | 0.002 | 0.003 | 0.003 | 0.005 | 0.007 | 0.017 | 0.027 | 13.443 | 26.728 |

**Fatigue damage/yr ($\times 10^{-5}$) in SCR TDZ**

For the vessel positioned in any of these stations, it could be seen that the associated fatigue damage occurring at other stations' critical arclength are quite negligible except for the immediate neighbouring station's critical arc length. This is the general behaviour of the fatigue damage responses considering other stations in any given relocation program. The effective fatigue damage ($D_{eff}$) is obtained by summing the SCR fatigue damage at each station ($D_m$) factored by the corresponding fatigue damage fraction ($f_m$) across all stations as presented in equation (12). For the index-225 relocation program, the $D_{eff}$ range graph maximum has already been presented in Figure 10. From Figure 10, it could be observed for the index-225 relocation program that the arc length where the maximum $D_{eff}$ occur is 1786.8m, which never

appear as a critical arc length for any of the 19 stations in Table 8. However, this arch length is very close to 1787.85m, which is the SCR TDZ critical fatigue damage arc length when the vessel is at station-8. It should be noted that this arclength is not the point that experienced the maximum fatigue damage across the stations. The maximum fatigue damage occurred at arclength 1772.8m when the vessel was at station-10 (see Table 8 and Figure 17). It is therefore evident that the point of maximum $D_{eff}$ for the relocation program is most likely not the point which experienced the highest fatigue damage across the stations. This generally applies to all relocation programs and presents the fatigue damage spreading basis either for a newly designed SCR or an existing SCR (for life extension purpose).

### 5.3. Vessel relocation cost

Although no cost objective function was included in the optimisation analysis in this work, it is worth mentioning that the higher the number of relocation station $(p)$, the lower will be the effective fatigue damage $(D_{eff})$, and the higher will be the number of vessel relocations $(n)$ (see equation (2)). The cost of vessel relocation operations will be expected to increase with $n$ over the SCR design life. Hence, the objective function to reduce $D_{eff}$ will be in competition with the cost objective function. A balance can be reached to maximise the benefit of the program in terms of $D_{eff}$ at optimum operation cost.

The index-225 relocation program, which is the best program in the analysis example in this paper, will not be the best if an objective cost function were to be included in the problem. In Table 9, we present a group of other feasible relocation programs (index-217, 218, 219, 220, 221, 222, 223, 224) having the same relocation axis $(\alpha)$ and span radius $(R)$ as index-225, but with varying number of stations $(p)$ (also see Table 6). The maximum effective fatigue damage in the SCR TDZ for these programs have been presented in Figure 23. We can see from Figure 23 that the relocation programs with higher $p$ are more effective for fatigue damage reduction than those with lower $p$. However, it should be noted that the SCR TDZ fatigue performance dropped very quickly with increasing $p$, as seen in Figure 23. The range graph maximum of $D_{eff}$ for these programs are presented in Figure 24.

**Table 9**. Order of performance of relocation programs with varying number of relocation stations, $p$

| Index | Order of Performance* | $R$ (%) | $\alpha$ (deg) | $p$ |
|---|---|---|---|---|
| No relocation | - | - | - | 1 |
| 217 | 311 | 5 | 30 | 3 |
| 218 | 195 | 5 | 30 | 5 |
| 219 | 122 | 5 | 30 | 7 |
| 220 | 43 | 5 | 30 | 9 |
| 221 | 15 | 5 | 30 | 11 |
| 222 | 9 | 5 | 30 | 13 |
| 223 | 4 | 5 | 30 | 15 |
| 224 | 2 | 5 | 30 | 17 |
| 225 | 1 | 5 | 30 | 19 |

*The order of performance is the relocation program's position (S/N) in Table 6. Note that only the first 35 best relocation program were presented in Table 6.

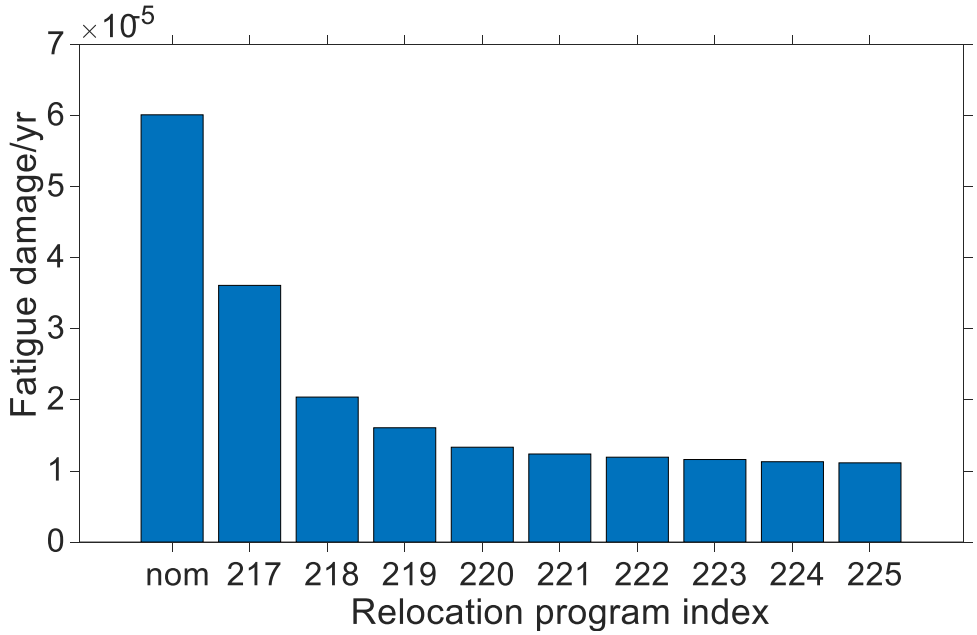


**Figure 23.** Maximum fatigue damage response with an increasing number of relocation station, $p$

These result plots show that the increasing cost associated with increasing $p$ will not be justified in terms of the fatigue performance when $p$ exceeds certain values. For example, for $p > 9$ (beyond index-220 relocation program), there is no appreciable improvement in the fatigue performance for the programs. Increasing the number of stations, $p$, beyond 9 will result in increased operating cost, but with no appreciable benefits to fatigue damage reduction in the SCR TDZ. Hence, an optimum relocation program should be selected vis-à-vis the associated vessel relocation operating cost during actual project relocation program design.

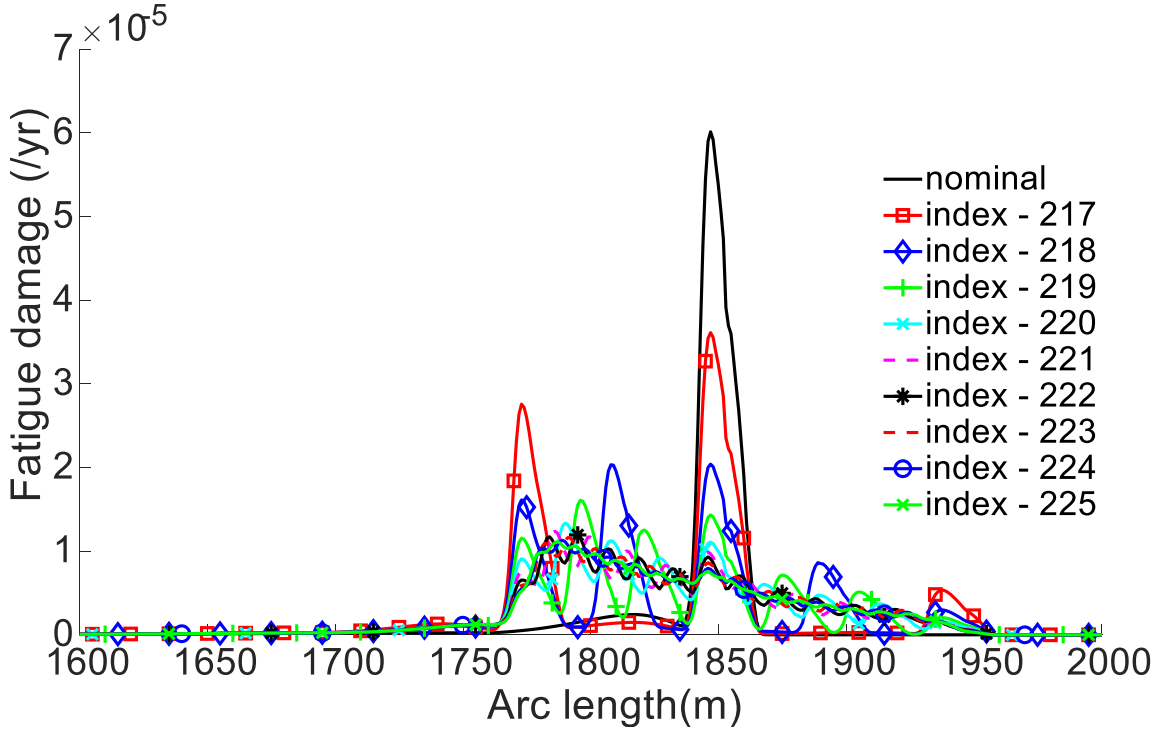


**Figure 24.** Range graph maximum of a family of relocation programs differing only in the number of relocation stations $p$.

## 6. CONCLUSION

The vessel relocation program involves managing, engineering, and operating the riser host floating vessel from one location or station to another. This may be required to enhance the spread of fatigue damage over a longer section of the SCR TDZ, resulting in effective reduction of the fatigue damage when compared with those of the SCRs with the host vessel not relocated. An approach to modelling vessel relocation is developed and presented in this paper. The relocation programs are modelled in terms of three optimisation design variables, which are the axis of relocation ($\alpha$), the span radius of relocation ($R$) and the number of relocation stations ($p$). An optimum combination of these variables can be obtained by casting the problem as an optimisation type, where the effective fatigue damage ($D_{eff}$) is the objective function and the SCR design storm responses (stress utilisation around TDZ ($U$), top tension ($T_{top}$) and TDZ compression ($T_{TDZ}$)) serve as the constraint function. In this paper, the index matching technique is applied to solve the optimisation problem. The methodology developed here is demonstrated using a single SCR hosted by an FPSO relocated symmetrically about the mean vessel position (nominal station).

The following can be deduced from the exampled vessel relocation optimisation analyses:

- The resulting SCR TDZ fatigue damage (effective damage, $D_{eff}$) from any relocation program depend on the exposure time and the configurations of the SCR. The configuration of the SCR is influenced by the combination of the design variables ($\alpha, R, p$)
- For a given $p$, the exposure time over the design life of the riser does not change irrespective of the $\alpha$ and the $R$. However, both $\alpha$ and $R$ affect the configuration of the risers, which in turn impacts the fatigue damage in the active SCR TDZ.
- Increasing $R$ will result in increased variation in the position of the fatigue hotspots in the active SCR TDZ, which will enhance the fatigue damage spreading and reduction in $D_{eff}$. However, $R$ is significantly limited by the constraint functions, which are the design storm responses of the SCR. Higher $R$ values can cause large compression, stress utilisation and fatigue damage in the SCR TDZ when the vessel is relocated to stations on the extreme near side of the riser.
- The optimum relocation axis ($\alpha$) may not necessarily be along the SCR plane axis as is generally expected.
- The reduction in the SCR TDZ fatigue damage increases with increasing $p$. However, the higher the value of $p$, the higher will be the number of relocations ($n$) of the vessel over the riser design life, and hence the increased cost of the relocation program. Therefore, a practical $p$ value should be selected with relocation cost consideration.

The analysis result for the single SCR case study shows that an SCR fatigue damage reduction up to 81% can be achieved with the vessel relocation program compared with the case where the vessel is not relocated. This indicates that the vessel relocation technique can provide significant fatigue performance for the SCRs if properly planned through optimisation. This benefit may not easily be achieved from the redesign (modification) of the TDZ section of the SCR. The vessel relocation technique provides ample opportunities to extend the life of the SCRs for brownfields. If considered during greenfield development, it can result in SCRs with reduced wall thickness and a consequent weight reduction. These benefits directly impact the

vessel and hang-off structure holding required capacities and the SCR cost. However, the operating cost associated with the vessel relocation program and the cost associated with the SCR TDZ modification need to be compared to inform the final decision on the SCR fatigue improvement options.

## RECOMMENDATION

Although a single SCR case is used to demonstrate the technique presented in this paper, this technique can be extended to multiple SCR of different azimuth, hang-off angle, and pipe geometry. In this study, a symmetric vessel relocation about the nominal station along the relocation axes is considered. However, a non-symmetric vessel relocation about the vessel's nominal station will allow candidate relocation programs that are not centred on the nominal FPSO position to be considered. This may provide further improvement of the effective fatigue damage performance. This approach is being explored in the ongoing vessel relocation optimisation study for vessel hosting multiple SCR systems.

## ACKNOWLEDGEMENTS

The authors acknowledge the support of the University of Strathclyde and McDermott International for this research. Numerical simulations in this work was performed using the ARCHIE-WeST High-Performance Computer (www.archie-west.ac.uk) based at the University of Strathclyde.

## REFERENCES

[1] C. M. Larsen and T. Hanson, "Optimisation of catenary risers," 1999.

[2] B. A. Carter and B. F. Ronalds, "Deepwater Riser Technology," in *SPE Asia Pacific Oil and Gas Conference and Exhibition*, 1998, vol. All Days, SPE-50140-MS, doi: 10.2118/50140-ms. [Online]. Available: https://doi.org/10.2118/50140-MS

[3] S. A. Hatton, "Update on the design of steel catenary riser systems," *TRANSACTIONS-INSTITUTE OF MARINE ENGINEERS-SERIES C-,* vol. 111, pp. 127-138, 1999.

[4] R. Song and P. Stanton, "Advances in Deepwater Steel Catenary Riser Technology State-of-the-Art: Part II—Analysis," in *ASME 2009 28th International Conference on Ocean, Offshore and Arctic Engineering*, 2009: American Society of Mechanical Engineers Digital Collection, pp. 285-296.

[5] E. Clukey, R. Ghosh, P. Mokarala, and M. Dixon, "Steel catenary riser (SCR) design issues at touch down area," 2007: International Society of Offshore and Polar Engineers.

[6] R. Song and P. Stanton, "Advances in Deepwater Steel Catenary Riser Technology State-of-the-Art: Part I—Design," in *International Conference on Offshore Mechanics and Arctic Engineering*, 2007, vol. 42673, pp. 331-344.

[7] H. Quintin, J.-L. Legras, K. Huang, and M. Wu, "Steel catenary riser challenges and solutions for deepwater applications," in *Offshore technology conference*, 2007: Offshore Technology Conference.

[8] J. R. Maison and J. F. Lea, "Sensitivity Analysis Of Parameters Affecting Riser Performance," presented at the Offshore Technology Conference, Houston, Texas, 1977/1/1/, 1977.

[9] L. M. Quéau, M. Kimiaei, and M. F. Randolph, "Sensitivity studies of SCR fatigue damage in the touchdown zone using an efficient simplified framework for stress range evaluation," *Ocean Engineering,* vol. 96, pp. 295-311, 2015.

[10] A. M. Ogbeifun, S. Oterkus, J. Race, H. Naik, E. Decnop, and M. Dakshina, "The Branched Riser Systems: Concept Development," in *ASME 2019 38th International Conference on Ocean, Offshore and Arctic Engineering*: American Society of Mechanical Engineers Digital Collection.

[11] R. K. Aggarwal *et al.*, "Development and Qualification of Alternative Solutions for Improved Fatigue Performance of Deepwater Steel Catenary Risers," in *ASME 2007 26th International Conference on Offshore Mechanics and Arctic Engineering*, 2007, vol. Volume 1: Offshore Technology; Special Symposium on Ocean Measurements and Their Influence on Design, pp. 315-329, doi: 10.1115/omae2007-29325. [Online]. Available: https://doi.org/10.1115/OMAE2007-29325

[12] S. Bhat, A. Dutta, J. Wu, and I. Sarkar, "Pragmatic Solutions to Touch-Down Zone Fatigue Challenges in Steel Catenary Risers," in *Offshore Technology Conference*, 2004: Offshore Technology Conference.

[13] R. K. Aggarwal, S. U. Bhat, T. S. Meling, C. van der Linden, M. M. Mourelle, and M. Else, "Qualification of enhanced SCR design solutions for improving fatigue life at touch down zone," in *The Sixteenth International Offshore and Polar Engineering Conference*, 2006: International Society of Offshore and Polar Engineers.

[14] A. M. Mansour, S. Bhat, D. Pasala, and D. Kumar, "Field Development using Semisubmersible Floating Production System with Steel Catenary Risers in Western Australia Harsh Environment," in *Offshore Technology Conference*, 2014, vol. Day 4 Thu, May 08, 2014, D041S052R007, doi: 10.4043/25265-ms. [Online]. Available: https://doi.org/10.4043/25265-MS

[15] P. Cao and J. Cheng, "Design of Steel Lazy Wave Riser for Disconnectable FPSO," in *Offshore Technology Conference*, 2013, vol. All Days, OTC-24166-MS, doi: 10.4043/24166-ms. [Online]. Available: https://doi.org/10.4043/24166-MS

[16] B. P. Jacob, M. C. Reyes, B. S. de Lima, A. L. Torres, M. M. Mourelle, and R. Silva, "Alternative configurations for steel catenary risers for turret-moored FPSOs," in *The Ninth International Offshore and Polar Engineering Conference*, 1999: International Society of Offshore and Polar Engineers.

[17] N. Alderton and R. Thethi, "Choosing the most appropriate rigid catenary riser design for various deepwater and harsh environments," *Advances in Riser Systems & Subsea Technologies for Deepwater Euroforum,* 1998.

[18] W. L. Alexander, M. Wu, and S.-H. M. Chang, "Dynamic Performance Comparison of Deepwater Riser Systems for A Turret-Moored FPS," in *Offshore Technology Conference*, 1999, vol. All Days, OTC-10934-MS, doi: 10.4043/10934-ms. [Online]. Available: https://doi.org/10.4043/10934-MS

[19] B. Thomas, A. Benirschke, and T. Sarkar, "Parque das Conchas (BC-10) Steel Lazy Wave Riser Installation: Pre-Abandonment, Recovery and Transfer Challenges," in *Offshore Technology Conference*, 2010, vol. All Days, OTC-20605-MS, doi: 10.4043/20605-ms. [Online]. Available: https://doi.org/10.4043/20605-MS

[20] E. Q. De Andrade, L. L. de Aguiar, S. F. Senra, E. F. N. Siqueira, A. L. F. L. Torres, and M. M. Mourelle, "Optimisation Procedure of Steel Lazy Wave Riser Configuration for Spread Moored FPSOs in Deepwater Offshore Brazil," in *Offshore Technology Conference*, 2010, vol. All Days, OTC-20777-MS, doi: 10.4043/20777-ms. [Online]. Available: https://doi.org/10.4043/20777-MS

[21] R. Franciss and E. Ribeiro, "Analyses of a Large Diameter Steel Lazy Wave Riser for Ultra Deepwater in Campos Basin," in *ASME 2004 23rd International Conference on*

*Offshore Mechanics and Arctic Engineering*, 2004, vol. 23rd International Conference on Offshore Mechanics and Arctic Engineering, Volume 1, Parts A and B, pp. 355-361, doi: 10.1115/omae2004-51176. [Online]. Available: https://doi.org/10.1115/OMAE2004-51176

[22] A. L. c. F. Lima Torres, E. C. Gonzalez, M. Q. de Siqueira, C. M. Silva Dantas, M. M. Mourelle, and R. M. Correia da Silva, "Lazy-Wave Steel Rigid Risers for Turret-Moored FPSO," in *ASME 2002 21st International Conference on Offshore Mechanics and Arctic Engineering*, 2002, vol. 21st International Conference on Offshore Mechanics and Arctic Engineering, Volume 1, pp. 203-209, doi: 10.1115/omae2002-28124. [Online]. Available: https://doi.org/10.1115/OMAE2002-28124

[23] M. M. Mourelle, M. Q. de Siqueira, G. G. de Avila, and A. L. F. L. Torres, "Methodology for Analysis of Installation of a Steel Lazy Wave Riser," in *2004 International Pipeline Conference*, 2004, vol. 2004 International Pipeline Conference, Volumes 1, 2, and 3, pp. 1945-1950, doi: 10.1115/ipc2004-0110. [Online]. Available: https://doi.org/10.1115/IPC2004-0110

[24] L. V. Sudati Sagrilo, E. Castro Prates de Lima, F. J. Mendes de Sousa, C. M. Silva Dantas, M. Q. de Siqueira, and A. L. c. Fernandes Lima Torres, "Steel Lazy Wave Riser Design: API-RP-2RD and DNV-OS-F201 Criteria," in *ASME 2005 24th International Conference on Offshore Mechanics and Arctic Engineering*, 2005, vol. 24th International Conference on Offshore Mechanics and Arctic Engineering: Volume 1, Parts A and B, pp. 107-113, doi: 10.1115/omae2005-67040. [Online]. Available: https://doi.org/10.1115/OMAE2005-67040

[25] F. E. Roveri, C. v. de Arruda Martins, and R. Balena, "Parametric Analysis of a Lazy-Wave Steel Riser," in *ASME 2005 24th International Conference on Offshore Mechanics and Arctic Engineering*, 2005, vol. 24th International Conference on Offshore Mechanics and Arctic Engineering: Volume 1, Parts A and B, pp. 289-295, doi: 10.1115/omae2005-67128. [Online]. Available: https://doi.org/10.1115/OMAE2005-67128

[26] A. L. c. F. Lima Torres, E. C. Gonzalez, M. D. A. da S. Ferreira, M. Q. de Siqueira, M. M. Mourelle, and R. M. Correia da Silva, "Lazy-Wave Steel Rigid Risers for FSO With Spread Mooring Anchoring System," in *ASME 2003 22nd International Conference on Offshore Mechanics and Arctic Engineering*, 2003, vol. Volume 2: Safety and Reliability; Pipeline Technology, pp. 547-555, doi: 10.1115/omae2003-37068. [Online]. Available: https://doi.org/10.1115/OMAE2003-37068

[27] P. A. Trapper, "Feasible numerical analysis of steel lazy-wave riser," *Ocean Engineering,* vol. 195, p. 106643, 2020.

[28] B. J. Elliott, A. Zakeri, A. Macneill, R. Phillips, E. C. Clukey, and G. Li, "Centrifuge modeling of steel catenary risers at touchdown zone part I: Development of novel centrifuge experimental apparatus," *Ocean Engineering,* vol. 60, pp. 200-207, 2013/03/01/ 2013, doi: https://doi.org/10.1016/j.oceaneng.2012.11.012.

[29] J. Wang, M. Duan, J. Fan, and Y. Liu, "Static Equilibrium Configuration of Deepwater Steel Lazy-Wave Riser," in *The Twenty-third International Offshore and Polar Engineering Conference*, 2013, vol. All Days, ISOPE-I-13-063.

[30] V. Jhingran, H. Zhang, H. Lie, H. Braaten, and J. K. Vandiver, "Buoyancy spacing implications for fatigue damage due to vortex-induced vibrations on a steel lazy wave riser (SLWR)," in *Offshore Technology Conference*, 2012: Offshore Technology Conference.

[31] A. Felisita, O. T. Gudmestad, D. Karunakaran, and L. O. Martinsen, "A Review of VIV Responses of Steel Lazy Wave Riser," no. 49934, p. V002T08A031, 2016, doi: 10.1115/OMAE2016-54321.

[32] A. Felisita, O. T. Gudmestad, D. Karunakaran, and L. O. Martinsen, "Review of steel lazy wave riser concepts for the north Sea," *Journal of Offshore Mechanics and Arctic Engineering,* vol. 139, no. 1, p. 011702, 2017.

[33] J. Murali and M. W. Joosten, "Titanium Drilling Risers—Application and Qualification," 2000.

[34] C. F. Baxter, R. W. Schutz, and C. S. Caldwell, "Experience and Guidance in the Use of Titanium Components in Steel Catenary Riser Systems," in *Offshore Technology Conference*, 2007, vol. All Days, OTC-18624-MS, doi: 10.4043/18624-ms. [Online]. Available: https://doi.org/10.4043/18624-MS

[35] M. Nygård, A. Sele, and K. Lund, "Design of a 25.5-in Titanium Catenary Riser for the Åsgard B Platform," in *Offshore Technology Conference*, 2000: Offshore Technology Conference.

[36] M. Randolph and P. Quiggin, "Non-linear hysteretic seabed model for catenary pipeline contact," in *ASME 2009 28th International Conference on Ocean, Offshore and Arctic Engineering*, 2009: American Society of Mechanical Engineers, pp. 145-154.

[37] E. Zargar, M. Kimiaei, and M. Randolph, "A new hysteretic seabed model for riser-soil interaction," *Marine Structures,* vol. 64, pp. 360-378, 2019.

[38] C. P. Aubeny and G. Biscontin, "Seafloor-riser interaction model," *International Journal of Geomechanics,* vol. 9, no. 3, pp. 133-141, 2009.

[39] F. Jamaludin and J. Koto, "Catenary Offset Buoyant Riser Assembly for Malaysian Deepwater," *Science and Engineering,* vol. 12, 2017.

[40] D. N. Karunakaran and R. Baarholm, "COBRA: An Uncoupled Riser System for Ultradeep Water in Harsh Environment," in *Offshore Technology Conference*, 2013: Offshore Technology Conference.

[41] T. Nurwanto, D. Karunakaran, and R. Franciss, "COBRA Riser Concept for Ultra Deepwater Condition," in *ASME 2013 32nd International Conference on Ocean, Offshore and Arctic Engineering*, 2013, vol. Volume 4B: Pipeline and Riser Technology, V04BT04A030, doi: 10.1115/omae2013-11161. [Online]. Available: https://doi.org/10.1115/OMAE2013-11161

[42] D. Karunakaran, H. Aasen, and R. Baarholm, "New Un-coupled Deepwater Riser Concept for Harsh Environment–Catenary Offset Buoyant Riser Assembly (COBRA)," in *Deepwater Offshore Technology Conference. New Orleans, USA*, 2011, pp. 11-13.

[43] C. E. Haveman, A. R. Cribbs, and J. D. Miller, "Global Benefits and Operational Challenges of Vessel Relocation," in *ASME 2015 34th International Conference on Ocean, Offshore and Arctic Engineering*: American Society of Mechanical Engineers Digital Collection.

[44] B. Yue, M. Campbell, D. Walters, H. Thompson, and K. Raghavan, "Improved SCR design for dynamic vessel applications," in *International Conference on Offshore Mechanics and Arctic Engineering*, 2010, vol. 49132, pp. 495-504.

[45] V. Vijayaraghavan *et al.*, "Large diameter steel catenary riser solutions for semi-submersible platforms in offshore Northwest Australia," in *Offshore Technology Conference*, 2015: Offshore Technology Conference.

[46] A. Izquierdo *et al.*, "Qualification of Weldable X65 Grade Riser Sections with Upset Ends to Improve Fatigue Performance of Deepwater Steel Catenary Risers," in *The Eighteenth International Offshore and Polar Engineering Conference*, 2008: International Society of Offshore and Polar Engineers.

[47] R. Brito, L. Aguiar, and V. Prado, "Technical Feasibility Study of Steel Catenary Risers for Pre-Salt Field Developments," presented at the OTC Brasil, Rio de Janeiro, Brazil, 2017/10/24/, 2017.

[48] A. G. Garmbis, P. Zumpano Jr, L. L. Aguiar, R. M. Brito, and D. A. Rade, "A Fracture Mechanics-Based Feasibility Study of Damped Steel Catenary Risers for Pre-Salt Field Developments," in *International Conference on Offshore Mechanics and Arctic Engineering*, 2019, vol. 58813: American Society of Mechanical Engineers, p. V05BT04A042.

[49] A. I. Garcia and H. M. Q. Carmona, "Seamless steel tube for use as a steel catenary riser in the touch down zone," ed: Google Patents, 2008.

[50] A. M. Horn, M. Hauge, P.-A. Rø stadsand, B. Bjø rnbakk, P. Dahlberg, and T. Fossesholm, "Cost Effective Fabrication of Large Diameter High Strength Titanium Catenary Riser," in *ASME 2002 21st International Conference on Offshore Mechanics and Arctic Engineering*, 2002, vol. 21st International Conference on Offshore Mechanics and Arctic Engineering, Volume 3, pp. 331-337, doi: 10.1115/omae2002-28445. [Online]. Available: https://doi.org/10.1115/OMAE2002-28445

[51] M. Matsuishi and T. Endo, "Fatigue of metals subjected to varying stress," *Japan Society of Mechanical Engineers, Fukuoka, Japan,* vol. 68, no. 2, pp. 37-40, 1968.

[52] D. Heffernan, "An introduction to the Python interface to OrcaFlex," *Orcina, Tech. Rep2016,* 2016.

[53] D. N. Veritas, "Offshore standard dnv-os-f101," *Submarine pipeline systems,* 2010.

[54] D. N. Veritas, "Recommended practice DNV-C203: Fatigue design of offshore steel structures," ed: DNV Oslo, 2010.

[55] D.-O. Standard, "F201, 2010," *Dynamic Risers. DNV: Norway*.

[56] Orcina, "Knowledge Based Article - Generating Spectral RAOs," 2018. [Online]. Available: www.orcina.com.

[57] W. Ruan, W. Dai, and J. Wu, "Study on motion transfer rule and extreme dynamic response of SCR's top-end heave excitation," *Journal of Marine Engineering & Technology,* pp. 1-14, 2019.

[58] B. Yue, M. Campbell, D. Walters, H. Thompson, and K. Raghavan, "Novel Technique for SCR Porch Location Screening," in *International Conference on Offshore Mechanics and Arctic Engineering*, 2010, vol. 49132, pp. 411-418.

[59] Y. Cheng, R. Song, B. Mekha, A. Torstrick, and H. Liu, "Compression assessment of deepwater steel catenary risers at touch down zone," in *International Conference on Offshore Mechanics and Arctic Engineering*, 2007, vol. 42673, pp. 345-353.